Author/s:
Scanlan, JL;Robin, C

Title:
Genetic characterization of candidate ecdysteroid kinases in Drosophila melanogaster

Date:
2024-11-01

Citation:
Scanlan, J. L. & Robin, C. (2024). Genetic characterization of candidate ecdysteroid kinases in Drosophila melanogaster. G3 Genes Genomes Genetics, 14 (11), https://doi.org/10.1093/g3journal/jkae204.

Persistent Link:
https://hdl.handle.net/11343/358536

G3, 2024, **14(11)**, jkae204
https://doi.org/10.1093/g3journal/jkae204
Advance Access Publication Date: 29 August 2024
Investigation

Genetic characterization of candidate ecdysteroid kinases in *Drosophila melanogaster*

Jack L. Scanlan, Charles Robin *

School of BioSciences, The University of Melbourne, Parkville Campus, Melbourne, Victoria 3010, Australia

*Corresponding author: School of BioSciences, The University of Melbourne, Building 184, Parkville Campus, Melbourne, Victoria 3010, Australia. Email: crobin@unimelb.edu.au

Ecdysteroids are major hormones in insects and control molting, growth, reproduction, physiology, and behavior. The biosynthesis of ecdysteroids such as 20-hydroxyecdysone (20E) from dietary sterols is well characterized, but ecdysteroid catabolism is poorly understood. Ecdysteroid kinases (EcKs) mediate the reversible phosphorylation of ecdysteroids, which has been implicated in ecdysteroid recycling during embryogenesis and reproduction in various insects. However, to date, only 2 EcK-encoding genes have been identified, in the silkworm *Bombyx mori* and the mosquito *Anopheles gambiae*. Previously, we identified 2 ecdysteroid kinase-like (EcKL) genes—*Wallflower* (*Wall*) and *Pinkman* (*pkm*)—in the model fruit fly *Drosophila melanogaster* that are orthologs of the ecdysteroid 22-kinase gene *BmEc22K*. Here, using gene knockdown, knockout, and misexpression, we explore *Wall* and *pkm*'s possible functions and genetically test the hypothesis that they encode EcKs. *Wall* and *pkm* null mutants are viable and fertile, suggesting that they are not essential for development or reproduction, whereas phenotypes arising from RNAi and somatic CRISPR appear to derive from off-target effects or other artifacts. However, misexpression of *Wall* results in dramatic phenotypes, including developmental arrest, and defects in trachea, cuticle, and pigmentation. *Wall* misexpression fails to phenocopy irreversible ecdysteroid catabolism through misexpression of *Cyp18a1*, suggesting that Wall does not directly inactivate 20E. Additionally, *Wall* misexpression phenotypes are not attenuated in *Cyp18a1* mutants, strongly suggesting that Wall is not an ecdysteroid 26-kinase. We hypothesize that the substrate of Wall in this misexpression experiment and possibly generally is an unknown, atypical ecdysteroid that plays essential roles in *Drosophila* development, and may highlight aspects of insect endocrinology that are as-yet uncharacterized. We also provide preliminary evidence that *CG5644* encodes an ecdysteroid 22-kinase conserved across Diptera.

Keywords: ecdysone; 20-hydroxyecdysone; 3-dehydroecdysone; trachea; UAS/GAL4; RNAi; CRISPR; steroid

Introduction

Ecdysteroids are polyhydroxylated steroids that control numerous aspects of insect biology, most notably molting, growth, and reproduction (Riddiford 1993). Twenty-hydroxyecdysone (20E) is responsible for most of the functions attributed to ecdysteroids, although its precursor ecdysone (E) may also have specific developmental roles (Beckstead *et al.* 2007; Ono 2014). The nuclear receptor heterodimer EcR/USP and the G protein-coupled receptor DopEcR are thought to modulate most genomic and non-genomic responses to ecdysteroids (Baker *et al.* 2000; Wang *et al.* 2000; Ishimoto *et al.* 2013), although the nuclear receptor DHR38 may also be involved in ecdysteroid signaling (Baker *et al.* 2003). The biosynthesis of ecdysteroids from dietary sterols involves the highly conserved "Halloween"? enzymes (Rewitz *et al.* 2006, 2007) and the tight transcriptional regulation of Halloween genes is essential for controlling insect growth and development (Yamanaka *et al.* 2013; Kannangara *et al.* 2021). However, relatively little is known about ecdysteroid inactivation through catabolism and how this is regulated.

Ecdysteroid inactivation can modulate ecdysteroid signaling by reducing levels of active hormone and/or producing inactive "storage"? forms that can be recycled into active hormones. This can play important roles in reproduction, where maternal- or mate-contributed storage hormones can influence early development or reproductive physiology, respectively (Sonobe and Ito 2009; Crocker and Hunter 2018; Peng *et al.* 2022). It can also function in development, by shaping the pulse-like titers of 20E required for developmental transitions (Rewitz *et al.* 2010). Ecdysteroid recycling might also be responsible for the mid-pupal pulse of 20E in some brachyceran dipterans (Ohtaki 1981; Scanlan *et al.* 2023), although this does not appear to be the case in *Drosophila melanogaster* (Zhang *et al.* 2024).

Ecdysteroid catabolic reactions can be broadly classified into modifications and conjugations. Modifications involve changes to various hydroxyl groups on the ecdysteroid nucleus. 26-Hydroxylation occurs via Cyp18a1 (Guittard *et al.* 2011) and can result in ecdysteroids that may be functional in some insects but not others (Kaplanis *et al.* 1973; Baker *et al.* 2000). 26-Hydroxylated ecdysteroids can be further oxidized by Cyp18a1 to 26-ecdysonoic acids, which is an irreversible process and widespread across taxa (Fig. 1; Rewitz *et al.* 2010; Li *et al.* 2014). 3-Oxidation and 3-epimerization also occur through ecdysteroid 3-oxidases and 3-alpha-reductases (Takeuchi *et al.* 2001; Sun *et al.* 2012), although the former modification can be reversed through the action of 3-beta-reductases (Sakurai *et al.* 1989; Chen *et al.* 1996). Conjugations involve the

Received on 20 January 2024; accepted on 26 June 2024

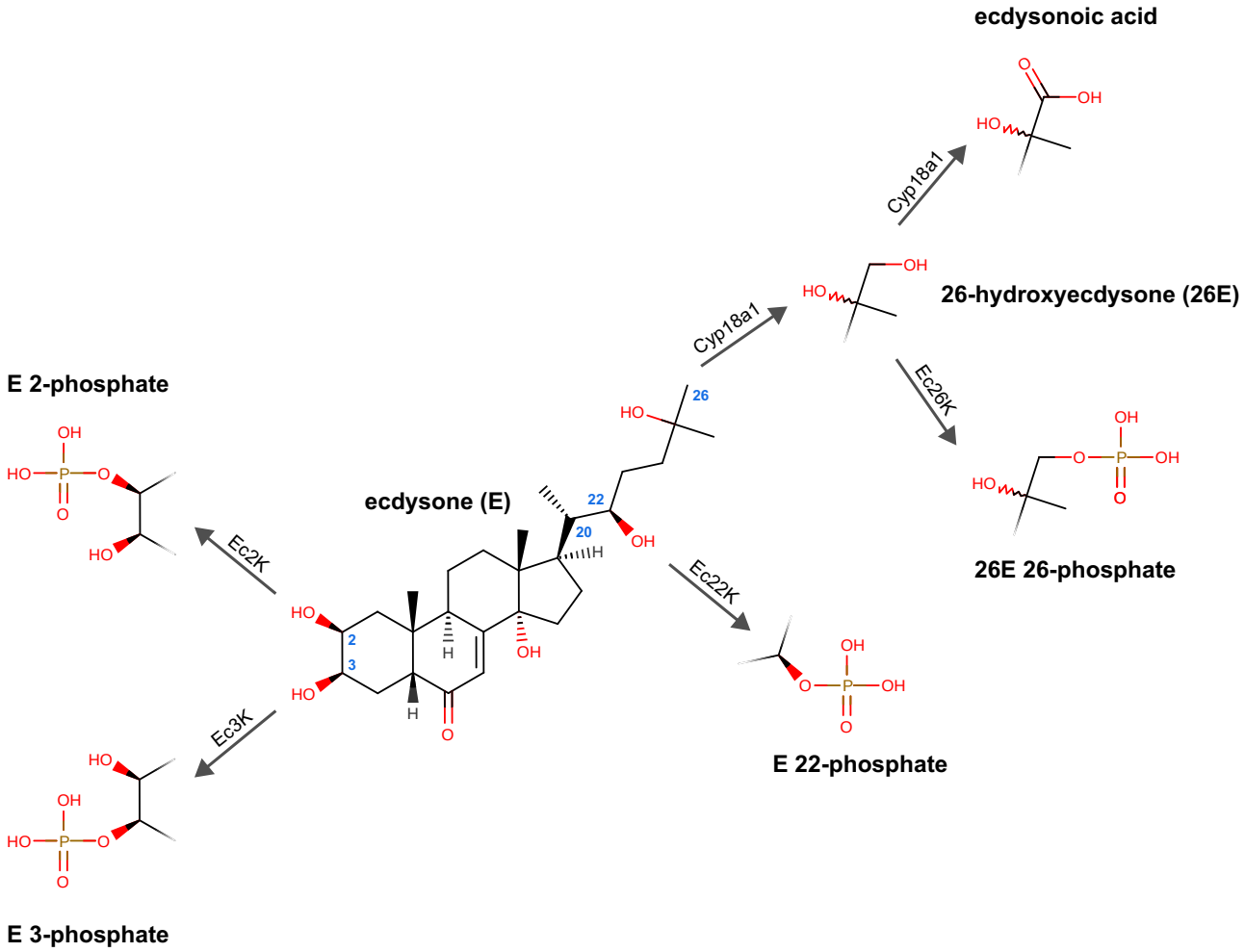

Fig. 1. Diagram of the four types of ecdysteroid phosphorylation reactions and their corresponding ecdysteroid kinase enzymes, and the hydroxylation and carboxylation reactions of Cyp18a1, based around the ecdysone nucleus. Key carbon positions are shown with small blue numbers on the ecdysone molecule.

addition of a bulky polar or nonpolar moiety that is thought to broadly limit the binding affinity to ecdysteroid receptors (Baker *et al.* 2000; Makka *et al.* 2002). Conjugated moieties include glucose (Thompson *et al.* 1987), fatty acids (Hoffmann *et al.* 1985), and acetate (Modde *et al.* 1984), although the most common is phosphate.

Phosphorylation reactions can occur at 4 potentially hydroxylated carbons on the ecdysteroid nucleus—C-2, C-3, C-22, and C-26 (Fig. 1)—but the prevalence of each seems to vary broadly across both substrates and taxa (reviewed in Lafont *et al.* 2012). Some ecdysteroid-phosphates can be hydrolyzed in vivo to active ecdysteroids through the action of phosphatases (Isaac, Sweeney, *et al.* 1983; Yamada and Sonobe 2003; Davies *et al.* 2007) but others may be non-hydrolyzable, and therefore terminal, catabolites (Lagueux *et al.* 1984; Sonobe and Yamada 2004).

The most well-defined function for ecdysteroid-phosphates in insect biology is ovary–embryo recycling: phosphate conjugates are formed in, or transported to, the oocyte and hydrolyzed to active hormones after fertilization. *Bombyx mori* (Lepidoptera: Bombycidae) recycle 22-phosphates of 20E and some precursors in its eggs (Sonobe and Ito 2009), while the related moth *Manduca sexta* (Lepidoptera: Sphingidae) recycles 26-hydroxy-E 26-phosphate (Feldlaufer *et al.* 1988). Two locust species, *Schistocerca gregaria* and *Locusta migratoria* (Orthoptera: Acrididae), both recycle ecdysteroid 22-phosphates (Isaac, Rose, *et al.* 1983; Isaac, Sweeney, *et al.* 1983; Lagueux *et al.* 1984). Hydrolysis of ecdysteroid-phosphates seems to control embryonic diapause in *B. mori* (Yamada *et al.* 2005; Matsushima *et al.* 2019) and may do the same in locusts (Tawfik *et al.* 2002). Various ecdysteroid-phosphates are also produced during later life stages of lepidopterans and orthopterans but their functions are unclear (Gibson *et al.* 1984; Modde *et al.* 1984; Beydon *et al.* 1987; Lozano *et al.* 1989).

In Diptera, ecdysteroid phosphorylation saw comparatively limited study until recently. In the mosquito *Anopheles gambiae* (Diptera: Culicidae), 3-dehydro-20E 22-phosphate is a male sexual gift that is dephosphorylated in the female reproductive tract to prevent remating (Peng *et al.* 2022). 20E is also converted to a 22-phosphate in virgin females of this species to modulate the hormonal response to blood-feeding (Peng *et al.* 2022). In *Musca domestica* (Diptera: Muscidae), ecdysteroid 2-phosphorylation can be induced by a synthetic ecdysteroid agonist but its physiological function remains unclear (Williams *et al.* 2002). In *D. melanogaster*, 4 ecdysteroid-phosphates have been identified: 3-dehydro-E 2-phosphate and 3-epi-20E 3-phosphate in larvae (Sommé-Martin *et al.* 1988a; Hilton 2004); E 22-phosphate in adult ovaries (Grau *et al.* 1995; Pis *et al.* 1995); and 20,26-dihydroxy-E 26-phosphate in the S2 cell line, due to the necessity of a phosphatase pretreatment when characterizing Cyp18a1 (Guittard *et al.* 2011). Possible roles for these metabolites in development or reproduction have yet to be identified.

Ecdysteroid-phosphate conjugates are produced by ecdysteroid kinases (EcKs); reverse genetic analyses of EcK genes could be a powerful method to understand the functions of ecdysteroid-phosphates in insect biology. To date, only 2 EcKs have been biochemically and genetically characterized: BmEc22K, which is responsible for ecdysteroid 22-phosphate production in the *B. mori* ovary (Sonobe *et al.* 2006); and AgEcK2, which produces 20E 22-phosphate in *A. gambiae* virgin females (Peng *et al.* 2022). Both *BmEc22K* and *AgEcK2* belong to the ecdysteroid kinase-like (EcKL) gene family. We recently performed a comprehensive phylogenomic analysis of the EcKL family in 140 insect genomes, classifying them into 13 subfamilies. *BmEc22K* and *AgEcK2* belong to the A and D subfamilies, respectively, making other genes in these clades strong a priori candidates for encoding EcKs (Scanlan and Robin 2024). *D. melanogaster* contains 2 subfamily A genes: *CG13813*—which we name *Wallflower* (*Wall*) in this study—and *Pinkman* (*pkm*), previously named *CG1561*. Both genes have been lost 2–3 times in Diptera but are otherwise conserved as single-copy orthologs in most species (Scanlan and Robin 2024), and they are more closely related to each other than they are to any lepidopteran subfamily A EcKL (Supplementary Fig. 1). *Wall* and *pkm* share 23 and 28% identity, and 42 and 47% identity, to *BmEc22K* along their alignable amino acid sequence, respectively (Supplementary Fig. 2).

pkm is strongly expressed in the adult eye, with some expression in the pupal CNS and fat body (Xu *et al.* 2004; Graveley *et al.* 2011; Leader *et al.* 2018). The Pkm protein has an N-terminal disordered domain, atypical of most EcKLs, and may physically interact with the small heat shock proteins Hsp23 and Hsp26 and an uncharacterized carbonyl reductase, CG11200 (Guruharsha *et al.* 2011). It has been proposed that Pkm modulates synapse formation through interactions with Hsp23 and Hsp26 (Santana *et al.* 2020). *pkm* also appears to be transcriptionally induced in adult oenocytes during starvation, under the control of insulin signaling (Chatterjee *et al.* 2014); given this, we hypothesize *pkm* has a role in the metabolic response to starvation.

Wall is primarily expressed in the midgut of embryos, larvae, and adult flies (Weiszmann *et al.* 2009; Leader *et al.* 2018). Despite a lack of focused study, multiple transcriptional data suggest that *Wall* has an ecdysteroid-related function. Specifically, *Wall* has: (1) enriched expression in the 3rd-instar larval ring gland (RG), which contains the ecdysteroidogenic prothoracic gland (PG) cells (Ou *et al.* 2016); (2) temporal co-expression with *Cyp18a1* (Graveley *et al.* 2011; Supplementary Fig. 3), especially during the mid-embryonic pulse of ecdysteroids (Maróy *et al.* 1988); (3) strong induction by exogenous 20E in nearly all surveyed cell lines (Gauhar *et al.* 2009; Stoiber *et al.* 2016); and (4) positive regulation by the primary 20E response gene *DHR3* (Ruaud *et al.* 2010; Mazina *et al.* 2015). Given that *Wall* is strongly expressed in S2 cells during 20E exposure and is co-expressed with *Cyp18a1* during embryogenesis, we hypothesize that *Wall* could encode the ecdysteroid 26-kinase proposed by Guittard *et al.* (2011).

Here, we genetically characterize the EcKL genes *pkm* and *Wall* through germline and somatic CRISPR knockouts, RNAi knockdown, and UAS–GAL4 misexpression. We also test 2 specific hypotheses: (1) that *Wall* encodes an ecdysteroid 26-kinase, through epistasis experiments with *Cyp18a1*; and (2) that *pkm* is involved in the starvation response in adult flies. We aim to genetically identify EcKs in *D. melanogaster*, in order to shed light on their functions in this species and across insects more broadly.

Materials and methods

Fly lines and husbandry

The following fly lines (BL, Bloomington line) were obtained from the Bloomington Drosophila Stock Center (BDSC): *w*;; Sb*^{1}/TM3 *actGFP Ser*^{1} (BL4534), *Tango11*^{1}/CyO *actGFP* (BL36320), FM7i *actGFP*/C(1)DX *y*^{1} *f*^{1} (BL4559), FM7*j* (BL6418), *y*^{1} *w*^{67c23};; *P{EPgy2}EY20330* (BL23106, called UAS-*Wall*^{EY} herein), *w**; *nos-GAL4*; UAS-*Cas9.P2* (BL67083), and *elav-GAL4*; UAS-*Cas9.P2*/CyO (BL67073). The following UAS-dsRNA (and control genotype) lines were obtained from the Vienna Drosophila Resource Centre (VDRC): VL60100 ("KK control"?), *w*^{1118} (VL60000; "GD control"?), *KK*^{Wall} (VL104249), *GD*^{Wall} (VL45409), *KK*^{pkm} (VL106503), *GD*^{pkm1} (VL32634), and *GD*^{pkm2} (VL32635). UAS-*Cyp18a1* (Guittard *et al.* 2011), UAS-*Dcr2*/CyO; *tub-GAL4*/TM6B, and some GAL4 driver stocks (Supplementary Table 2) were a kind gift of Philip Batterham (The University of Melbourne). *w**; *tub-GAL80*^{ts}; TM2/TM6B and *y*^{1} *w* P{lacW}Fas2G0032 P{neoFRT}19A*/FM7c; *P{ey-FLP.N}5* were a kind gift of Michael Murray (The University of Melbourne). The strong loss-of-function *Cyp18a1*^{1} allele was described in Rewitz *et al.* (2010); a *Cyp18a1*^{1}/FM7i *actGFP* line was a kind gift of Michael O'Connor (University of Minnesota). For GAL4 driver lines used in this study, see Supplementary Table 1; other fly lines were made by routine crossing (Supplementary Methods).

For routine stock maintenance, flies were kept on yeast-cornmeal-molasses media ("lab media"?; http://bdsc.indiana.edu/information/recipes/molassesfood.html) at 18°C, 21°C, or 25°C in plastic vials sealed with cotton stoppers.

Generation of UAS-ORF lines

Cloning of ORFs into the pUASTattB vector (Bischof *et al.* 2007) and *D. melanogaster* transformation was as described in Scanlan *et al.* (2022), with the following modifications. The *Wall* ORF was isolated by PCR from the DGRC cDNA clones IP11764 and GH09153, using the primer pair CG13813_EagIF and CG13813_KpnIR (Supplementary Table 2). The 2 ORFs of *pkm*—the full 635 aa ORF ("*pkm*^{F}"?) and a truncated 430 aa ORF without the N-terminal intrinsically disordered region ("*pkm*^{T}"?)—were synthesized by Integrated DNA Technologies, with *EagI* and *KpnI* restriction sites (plus 6 additional nucleotides to allow for efficient digestion) at the N- and C-termini, respectively. Expected amplicon sizes from recombinant plasmids in colony PCR for *Wall*, *pkm*^{F}, and *pkm*^{T} were 1,521 bp, 2,136 bp, and 1,521 bp, respectively (using primers pUASTattB_3F and pUASTattB_5R; Supplementary Table 2). All correctly assembled plasmids, as verified by Sanger sequencing, were sent to TheBestGene Inc. (USA) for microinjection and incorporation into the *D. melanogaster* genome at the attP40 site on chromosome 2 (BL25709).

Generation of mutants by CRISPR-Cas9

The recombinant pCFD6 plasmids pCFD6-CG13813 and pCFD6-CG1561—each of which express, under the control of a UAS promoter, 4 gRNAs that target either the *CG13813*/*Wall* locus (Fig. 2a) or the *CG1561*/*pkm* locus (Fig. 2b)—were designed in silico using Benchling (http://benchling.com), and cloned as described in Scanlan *et al.* (2022), with the following modifications: the primer pairs for the amplification of the inserts for pCFD6-CG13813 were pCFD6_CG13813_1F/R, pCFD6_CG13813_2F/R, and pCFD6_CG13813_3F/R; and the primer pairs for the amplification of the inserts for pCFD6-CG1561 were pCFD6_CG1561_1F/R, pCFD6_CG1561_2F/R, and pCFD6_CG1561_3F/R (Supplementary Table 2). Correctly assembled plasmids, as verified by Sanger sequencing, were sent to TheBestGene Inc. for microinjection and incorporation into the *D. melanogaster* genome at the attP40 site on chromosome 2 (BL25709), to produce the homozygous fly lines UAS-*Wall*^{pCFD6} and UAS-*pkm*^{pCFD6}.

Mutagenesis of the *Wall* locus on chromosome 3L followed protocols previously described in Scanlan *et al.* (2022), using the crossing scheme in Supplementary Fig. S4A. Mutagenesis of the *pkm* locus on the X chromosome was done using the crossing scheme

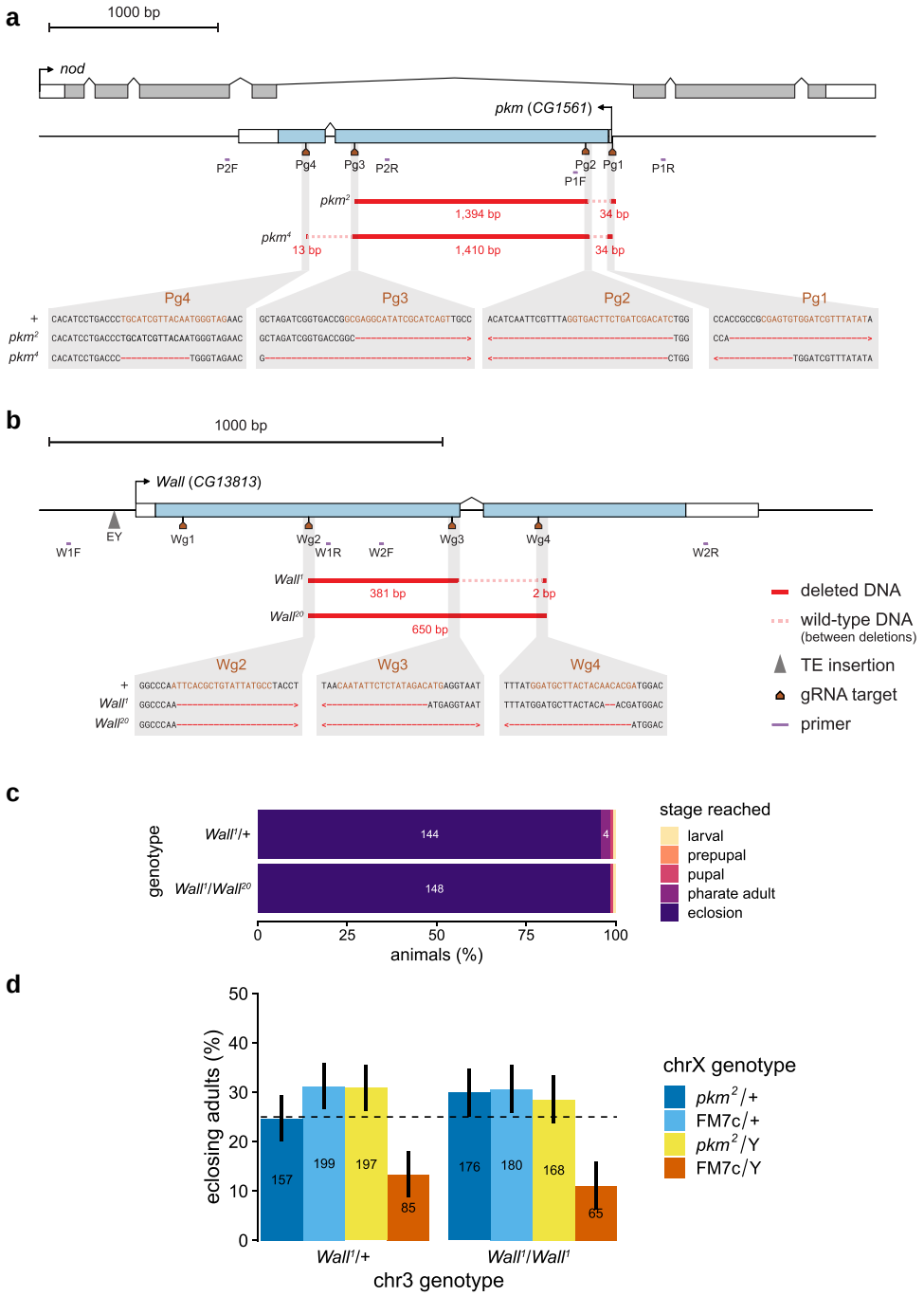

Fig. 2. CRISPR-Cas9 mutagenesis of *pkm* and *Wall*. a) The *Pinkman/pkm* (CG1561) locus on the X chromosome of *Drosophila melanogaster*, including the *pkm* gene (blue coding regions) and the *nod* gene (gray coding regions). Mapped onto the locus are the locations of gRNA target sites (Pg1–4; brown), genotyping primer-binding sites (purple), and 2 CRISPR-Cas9-induced deletion alleles (pkm^2 and pkm^4; deletion sizes in red text). P1F, ΔD37_1F; P1R, ΔD37_1R; P2F, ΔD37_2F; P2R, ΔD37_2R. b) The *Wallflower/Wall* (CG13813) locus on chromosome 3L of *Drosophila melanogaster*. Mapped onto the locus are the locations of gRNA target sites (Wg1–4; brown), genotyping primer-binding sites (purple), the *EYgp2* element EY20330 (gray triangle), and 2 CRISPR-Cas9-induced deletion alleles ($Wall^1$ and $Wall^{20}$; deletion sizes in red text). Neither deletion allele had lesions at the Wg1 target site. W1F, ΔD38_1F; W1R, ΔD38_1R; W2F, ΔD38_2F; W2R, ΔD38_2R. Wild-type DNA present in-between deletions is indicated with pale dashed lines. Gray boxes (bottom) are sequence-level detail of the deletions with respect to the wild-type genetic background (+). gRNA target sites are highlighted in brown, and deleted bases are red dashes; > and < symbols indicate that the deletion continues out of the frame of the highlighted sequence. c and d) Developmental viability of *Wall* and *pkm* single and double mutant animals. c) Larval-to-adult viability of offspring from crosses between $Wall^1$ females and wild-type (+) males (top) or $Wall^{20}$ males (bottom). Numbers on the bars are the number of individuals in each lethal phase category (for numbers greater than 3). d) Eclosing adult genotypic ratios of the offspring from crosses between pkm^2/FM7c;; $Wall^1$ females and $Wall^1$ (left) or w^{1118} (right) males. Bars are colored by their chrX genotype, as determined by their sex and the presence or absence of the FM7c balancer chromosome; pkm^2 hemizygotes are in yellow (single mutants on left, double mutants on right). The dashed line indicates the expected 1:1:1:1 genotypic ratio if all genotypes per cross are equally developmentally viable. Numbers on the bars are the number of adults of each genotype. Error bars are 97.5% confidence intervals (95% CI adjusted for 2 tests) for the proportion of each genotype within each cross.

in Supplementary Fig. S4B. Single founder female flies during *pkm* mutagenesis were allowed to lay viable larvae before undergoing DNA extraction.

Wall PCR genotyping used the ΔD38_1F/1R and ΔD38_2F/2R primer pairs, which produce amplicons of size 698 and 845 bp, respectively, from wild-type chromosomes, and ΔD38_1F/2R, which produce 1,689 bp amplicons from wild-type chromosomes and amplicons between ~700 and 1,500 bp in the case of deletions between any 2 *Wall* gRNA pairs. *pkm* PCR genotyping used the ΔD37_1F/1R and ΔD37_2F/2R primer pairs, which produce amplicons of size 693 and 898 bp, respectively, from wild-type chromosomes, and ΔD37_2F/1R, which produce 2,757 bp amplicons from wild-type chromosomes and amplicons between ~900 and 2,600 bp in the case of deletions between any 2 *pkm* gRNA pairs. PCR—2 min initial denaturation (95°C), then 2 min denaturation (95°C), 45 s annealing (55°C) and 1.5 min extension (72°C) for 32 cycles, and then a 5 min final extension (72°C)—was carried out with GoTaq Green Master Mix (Promega). Deletion loci from mutant flies were amplified using the genotyping primers above with 4 GoTaq Green PCR reactions per line, which were combined before gel-purification to allow for the detection of early-cycle polymerase-derived errors by close inspection of the sequencing chromatogram output. Gel-purified amplicons were sequenced using the appropriate genotyping primers at AGRF and compared to the *D. melanogaster* r6 reference genome at FlyBase (Gramates *et al.* 2022; Öztürk-Çolak *et al.* 2024).

Germline knockout, somatic knockout, RNAi knockdown, and misexpression developmental viability assays

Egg-to-adult and larval-to-adult viability assays were conducted as described in Scanlan *et al.* (2022), but at 25°C or 29°C depending on the experiment. The "MultinomCI"? function in the *DescTools* package in R was used to calculate confidence intervals for multinomial proportions.

Misexpression phenotyping was conducted by crossing 3–5 UAS-responder females to *GAL4* males, letting them lay in lab media vials for 24 h, with a minimum of 3 replicate vials per genotype; vials were left to develop at 25°C and were checked every 24 h for developmental arrest phenotypes. Arrest phenotypes were fully penetrant unless otherwise noted.

Delayed-onset misexpression assay

Three groups of 10 *act-GAL4*/CyO *actGFP* virgin females were crossed to *tub-GAL80^{ts}*; UAS-*Wall^{EY}* males and allowed to mate in lab media vials at 18°C for 24 h, then transferred to 3 fresh vials at 18°C (the GAL80^{ts} restrictive temperature) and allowed to lay for 24 h. This transfer-and-lay process was repeated every 24 h (with fresh females added after 9 days) until 19 sets of 3 vials containing offspring were produced, and then all the vials were shifted to 29°C (the GAL80^{ts} permissive temperature) to complete development—each set of vials contained animals that started expressing *Wall^{EY}* at a different developmental stage. Eclosing adults were genotyped based on the presence or absence of the phenotypic markers on the CyO *actGFP* chromosome. Adult genotype counts from each set of vials were analyzed by the "binom.test"? function in R (with a Bonferroni correction for multiple tests) to determine if genotypic ratios were significantly different from the Mendelian expectation (1:1).

Food avoidance assay

tub-GAL80^{ts}; *da-GAL4* virgin females were crossed to *w^{1118}* or UAS-*Wall^{EY}* males and laid eggs on juice plates (Supplementary Methods) at 25°C for 8 h. First-instar larvae were transferred to lab media vials (20 larvae per vial, 8 vials per genotype) and kept at 29°C. Two and 3 days post-hatching, the number of larvae located in the food substrate (mouthparts hidden in substrate; "digging"?), on top of the food substrate (mouthparts out of substrate; "on food"?), or on the sides of the vials (body completely off substrate; "side of vial"?) was scored for each genotype. Fisher's exact test was used to determine if there were significant differences in larval position between genotypes and/or timepoints, using the "fisher.test"? function in R.

Misexpression epistasis assays

Six *Cyp18a1^{1}*/FM7i *actGFP*; UAS-*Wall^{pU}* virgin females or +; UAS-*Wall^{pU}* virgin females were crossed to *da-GAL4* or *Mef2-GAL4* males and allowed to lay in lab media vials for 24 h, with 10 vials per genotype. Offspring were left to develop at 25°C for 14 days, and the number of individuals that reached pupariation, pupation (or pupariation/pupation for *da-GAL4* crosses), pharate adult differentiation, and eclosion were scored. Fisher's exact test was used to determine if there were significant differences between the developmental outcomes of offspring of each maternal genotype, using the "fisher.test"? function in R.

Starvation assays

Starvation assays were conducted at 21–22°C using the "wet starvation"? method developed by Storelli *et al.* (2019). Adult flies were collected as virgins in the first 12 h post-eclosion, separated by sex and kept in lab media vials for 2–3 days. Empty vials were half-filled with deionized water and cellulose acetate stoppers (Flystuff, 49–102) were pushed to the bottom and saturated. Excess water was thoroughly removed and 9–10 flies were placed into each vial (6 vials per sex-genotype combination), which were closed with an additional dry stopper. Flies were moved to fresh vials twice a week. Survival was scored every 24 h until all flies were dead. Male and female flies were analyzed separately due to known sex differences in starvation resistance (Jang and Lee 2015). Survival analysis was conducted with the *survival* (v2.38) and *survminer* (v0.4.7) packages in R, using a log-rank test to compare survival curves; pairwise *P*-values were adjusted for multiple tests using the Benjamini–Hochberg procedure.

Additional misexpression assays

UAS-ORF responder lines for 13 EcKLs were obtained from FlyORF at the University of Zurich (Bischof *et al.* 2013) or the DPiM transgenic fly resource at the Bangalore Fly Resource Center (Guruharsha *et al.* 2012); FlyORF lines contain 3xHA-tagged ORFs, while DPiM lines contain FLAG-HA-tagged ORFs. FlyORF EcKL lines used were F002982 (*CG31300*), F002821 (*CG10560*), F002832 (*CHKov2*; "*CHKov2^{1}*"?), and F002521 (*CG9259*). DPiM lines used were 817 (*CG10562*), 854 (*CHKov2*; "*CHKov2^{2}*"?), 1332 (*JhI-26*), 2262 (*CG14314*), 2439 (*CG5644*), 2866 (*CG10514*), 3380 (*CG6830*), 3774 (*CG31102*), 3915 (*CG31087*), and 3916 (*CG31288*). *w^{1118}* (VDRC stock 60000) was used as a wild-type control in the absence of true matched genetic backgrounds. *tub-GAL4*/TM3 *actGFP Ser^{1}* and *phm-GAL4*/CyO *actGFP* (Guittard *et al.* 2011) were a kind gift of Philip Batterham (The University of Melbourne).

UAS-ORF responder (and *w^{1118}*) males were crossed to *tub*-GAL4/TM3 *actGFP Ser^{1}* females, which were allowed to lay on lab media food, and the offspring were left to develop at 25°C for 14 days. Adult offspring were collected after eclosion and scored for the presence or absence of the TM3 *actGFP Ser^{1}* balancer chromosome (and the TM6B *Antp^{Hu} Tb^{1}* chromosome in the case of DPiM line 3774). UAS-*CG5644* males were also crossed to *phm-GAL4*/CyO *actGFP*

females; adult offspring were scored for the presence or absence of the CyO *actGFP* chromosome. The "binom.test"? function in R was used to test deviations from expected Mendelian ratios (1:1 for all crosses except those involving DPiM line 3774, which was 1:3)—significant deviations against misexpression genotypes were considered evidence for developmental lethality due to misexpression of the EcKL ORF in question.

Results

Pkm null mutants have no obvious developmental phenotypes, in contrast to somatic knockout and some RNAi knockdown animals

We explored the developmental essentiality of *pkm* through 3 gene disruption methods: germline CRISPR, to generate heritable null alleles; somatic CRISPR, to induce gene knockout in somatic tissues; and transgenic RNAi, to knock down mRNA levels. Through germline CRISPR mutagenesis, 18 putative deletions at the *pkm* locus were generated from 24 founder females. Two *pkm* composite deletion alleles were kept as homozygous-viable stocks and molecularly characterized: pkm^{2} and pkm^{4}. pkm^{2} comprises 2 deletions, one of 34 bp overlapping the transcription start site and another of 1,394 bp that induces a frameshift in exon 1, while pkm^{4} comprises 3 deletions, one of 34 bp that removes the transcription start site, one of 1,410 bp in-frame in exon 1, and another of 13 bp that induces a frameshift in exon 2 (Fig. 2a). Both alleles delete the ATP-binding Brenner's motif (Supplementary Fig. 2), induce frameshifts, and delete significant portions of the coding sequence, and are therefore likely strong loss-of-function (null) alleles.

The developmental essentiality of *pkm* was tested with egg-to-adult viability assays involving null mutants. In crosses between pkm^{2}/FM7c females and +/Y males, while FM7c hemizygotes appeared much less viable than other genotypes, there were no clear differences between the proportions of other genotypes, showing that pkm^{2}/Y hemizygotes are developmentally viable (Fig. 2d).

Somatic knockout of *pkm* using the ubiquitous *da-GAL4* driver resulted in a substantial number of adults falling into the food media, being unable to remove themselves and "drowning"?; these adults were unable to be easily counted. Tipping vials upside-down before eclosion revealed that knockout adults eclosed in a 1:1 ratio with balancer adults, indicating they had no detectable pre-adult lethality (Supplementary Fig. S5B), but had an uncoordinated limb phenotype, effectively resulting in immobility (Supplementary Fig. S5C), a phenotype not seen in *pkm* null mutants. This immobility phenotype was also observed when UAS-pkm^{pCFD6} and UAS-*Cas9* were driven with the (nonspecific; see Berger *et al.* 2007; Casas-Tintó *et al.* 2017) neuronal driver *elav-GAL4*, although this was not quantified.

RNAi knockdown experiments using the strong ubiquitous *tub-GAL4* driver were previously performed at 25°C with KK library UAS-*dsRNA* lines (Scanlan *et al.* 2020), but we added to this experiment by also using independently generated GD lines that target different parts of each gene's transcript (Dietzl *et al.* 2007). We also performed knockdown at a higher temperature (29°C), which increases GAL4 activity and should result in stronger knockdown (Fortier and Belote 2000; Duffy 2002), as well as at 29°C with the addition of a UAS-*Dcr2* transgene, which can further increase knockdown efficiency (Dietzl *et al.* 2007). For *pkm*, none of the 3 RNAi constructs produced detectable developmental arrest at 25°C (Supplementary Fig. S6A), but KK^{pkm} produced partially penetrant lethality before the adult stage at 29°C (Supplementary Fig. S6B). KK^{pkm}, GD^{pkm1}, and GD^{pkm2} all had significant effects on developmental viability compared to controls (all $P < 2.2 \times 10^{-16}$, Fisher's exact test) at 29°C when paired with the UAS-*Dcr2* transgene, with KK^{pkm} resulting in pupal and pharate adult lethality, and GD^{pkm1} and GD^{pkm2} producing a mix of pharate adult lethality and a "drowning"? phenotype whereby adults eclosed from the puparium but fell to the bottom of the vial and failed to escape from the semi-liquid food media (Supplementary Fig. S6D).

Wall null mutants and somatic knockout animals have no obvious developmental phenotypes, in contrast to most RNAi knockdown animals

We also explored the developmental essentiality of *Wall* through germline CRISPR, somatic CRISPR, and transgenic RNAi. Through germline CRISPR mutagenesis, 22 putative deletions at the *Wall* locus were detected by PCR from 66 founder males. Two *Wall* deletion alleles were kept as homozygous-viable stocks and molecularly characterized: $Wall^{1}$ and $Wall^{20}$. $Wall^{1}$ comprises 2 deletions in the coding region of the genes—a 381 bp in-frame deletion in exon 1 (between sgRNAs Wg2 and Wg3), and a 2 bp frameshift deletion in exon 2 (at sgRNA Wg4). $Wall^{20}$ comprises a single 605 bp frameshift deletion that spans exons 1 and 2 (Fig. 2b). Both alleles are predicted to significantly disrupt the function of the encoded protein, due to the deleted coding sequence (including Brenner's motif; Supplementary Fig. 2) and frameshifts, and are therefore likely also null alleles.

The developmental essentiality of *Wall* was tested with larval-to-adult viability assays involving null mutants. There were no significant differences between the developmental outcomes of $Wall^{1}$/+ and $Wall^{1}/Wall^{20}$ heterozygotes ($P = 0.152$, Fisher's exact test; Fig. 2c), with nearly all individuals successfully eclosing as viable adults. To test for possible developmental redundancy between *Wall* and *pkm*, we also conducted egg-to-adult viability assays with crosses that produced double mutant animals and compared the results to those that produced *pkm* single mutants (see above). There was no significant difference in the genotypic ratios between $Wall^{1}/Wall^{1}$ and $Wall^{1}$/+ crosses ($P = 0.168$, Fisher's exact test; Fig. 2d), demonstrating that double mutants (homozygous for $Wall^{1}$ and hemizygous for pkm^{2}) do not suffer any developmental viability loss compared to other genotypes.

We also noted that all generated *Wall* and *pkm* mutant stocks could be kept for multiple generations as viable homozygous stocks without obvious issues, suggesting that neither gene is required for fertility, although this was not quantified.

Somatic knockout of *Wall* produced no detectable loss of egg-to-adult viability compared to non-gRNA-expressing animals (Supplementary Fig. S5A), consistent with the viability of germline null mutants. In contrast, most RNAi knockdowns of *Wall* affected developmental progression. The KK^{Wall} RNAi construct (but not GD^{Wall}) resulted in detectable developmental arrest before the adult stage at either 25°C (Supplementary Fig. S6A) or 29°C (Supplementary Fig. S6B). Both KK^{Wall} and GD^{Wall} had significant effects on developmental viability compared to controls (both $P < 2.2 \times 10^{-16}$, Fisher's exact test) at 29°C when paired with the UAS-*Dcr2* transgene, with KK^{Wall} resulting in mostly larval lethality, and GD^{Wall} resulting in both pharate adult lethality and the "drowning"? phenotype seen with GD^{pkm1} and GD^{pkm2} knockdowns (Supplementary Fig. S6D).

RNAi-induced developmental arrest may be due to off-target effects, not genetic compensation

We considered our knockdown results to be suspicious, given that no developmental phenotypes were detected for *Wall* and *pkm* null mutant animals (Fig. 2c and d). However, discrepancies between null mutant and RNAi knockdown animals can be due "genetic compensation"?, wherein gene knockout triggers a compensatory mechanism (such as the up-regulation of genes with similar functions) to restore a wild-type phenotype, while RNAi knockdown fails to trigger

compensation, leading to a mutant phenotype (El-Brolosy and Stainier 2017; El-Brolosy *et al.* 2019). To test the hypothesis that the phenotypic discrepancy between knockdown animals and null mutant animals was due to genetic compensation in mutants, we performed *pkm* knockdown in a pkm^2 null mutant background, with the expectation that if genetic compensation was occurring in mutants, knockdown would fail to produce a developmental arrest phenotype, while if the knockdown phenotype was due to off-target effects, the presence of the pkm^2 allele would have no effect on the phenotype. Females homozygous for the KK^{pkm} construct—and homozygous for either the pkm^2 allele (1 of 2 such independently generated lines) or a wild-type allele (pkm^+)—were crossed to *tub-GAL4*/TM3, *actGFP*, Ser^1 males, and adult genotypic ratios of the offspring were scored, with half of the knockdown individuals (males) expected to be pkm^+ or pkm^2 hemizygotes. The proportion of adult knockdown individuals between knockdown crosses with pkm^+ and pkm^2 was not significantly different (Supplementary Fig. S6C), with a pkm^2 (line 1) vs pkm^+ odds ratio of 1.67 (97.5% CI: 0.94, 3.0) and a pkm^2 (line 2) vs pkm^+ odds ratio of 1.02 (97.5% CI: 0.54, 1.91). This demonstrates that the presence or absence of *pkm* loss-of-function alleles does not affect the *tub* > KK^{pkm} knockdown phenotype, strongly suggesting that these phenotypes are due to off-target effects and not genetic compensation.

A summary of all *pkm* and *Wall* knockout and knockdown phenotypes, for easy comparison, is presented in Supplementary Table 3.

Ubiquitous misexpression of *Wall*, but not *pkm*, causes developmental arrest

Without obvious requirements for *Wall* or *pkm* during development, we sought to test the hypothesis that these genes encode EcKs by misexpression, by driving UAS-ORF constructs (and an EPgy2 insertion upstream of the native *Wall* locus that contains a UAS and promoter region—UAS-$Wall^{EY}$) with the strong ubiquitous driver *tub-GAL4* at 25°C to explore if ectopic expression arrested developmental progression. As a positive control for ecdysteroid inactivation, we used a UAS-*Cyp18a1* responder (Guittard *et al.* 2011) to misexpress the ecdysteroid 26-hydroxylase/carboxylase Cyp18a1, which phenocopies mutations in the ecdysteroid biosynthetic pathway (Rewitz *et al.* 2010; Guittard *et al.* 2011).

Ubiquitous misexpression of *Cyp18a1* with *tub-GAL4* completely arrested development, as expected, as did ubiquitous misexpression of *Wall* with either the UAS-$Wall^{EY}$ line or the UAS-$Wall^{pU}$ line (Fig. 3a). Examination of offspring vials under a fluorescent microscope (to detect the presence of the TM3 *actGFP* Ser^1 balancer chromosome) suggested that these misexpression genotypes failed to complete embryogenesis and hatch as larvae. Misexpression of either of the *pkm* ORF transgenes failed to significantly alter adult genotypic ratios from Mendelian expectations (Fig. 3a), suggesting that ubiquitous expression of either *pkm* ORF does not affect developmental progression.

Misexpression of *Wall* using UAS-$Wall^{EY}$ and the strong, ubiquitous *act-GAL4* driver at 25°C also caused complete developmental arrest ($n = 158$ adults, $P < 2.2 \times 10^{-16}$, exact binomial test), although not all animals died as embryos, with some larvae hatching but dying before pupariation, with various morphological phenotypes, such as spiracle and rectal pad pigmentation, and tracheal and denticle belt defects (Fig. 3b–i).

Ubiquitous misexpression of *Wall* causes developmental arrest until the middle of metamorphosis

While ubiquitous misexpression of *Wall* was embryonic lethal and occasionally larval lethal, it was unclear if misexpression affected later developmental stages. To investigate this, a delayed-onset misexpression experiment was conducted using the temperature-sensitive *tub-GAL80*^{ts} construct, which represses GAL4 activity at 18°C and permits GAL4 activity at 29°C, and the *act-GAL4* driver,

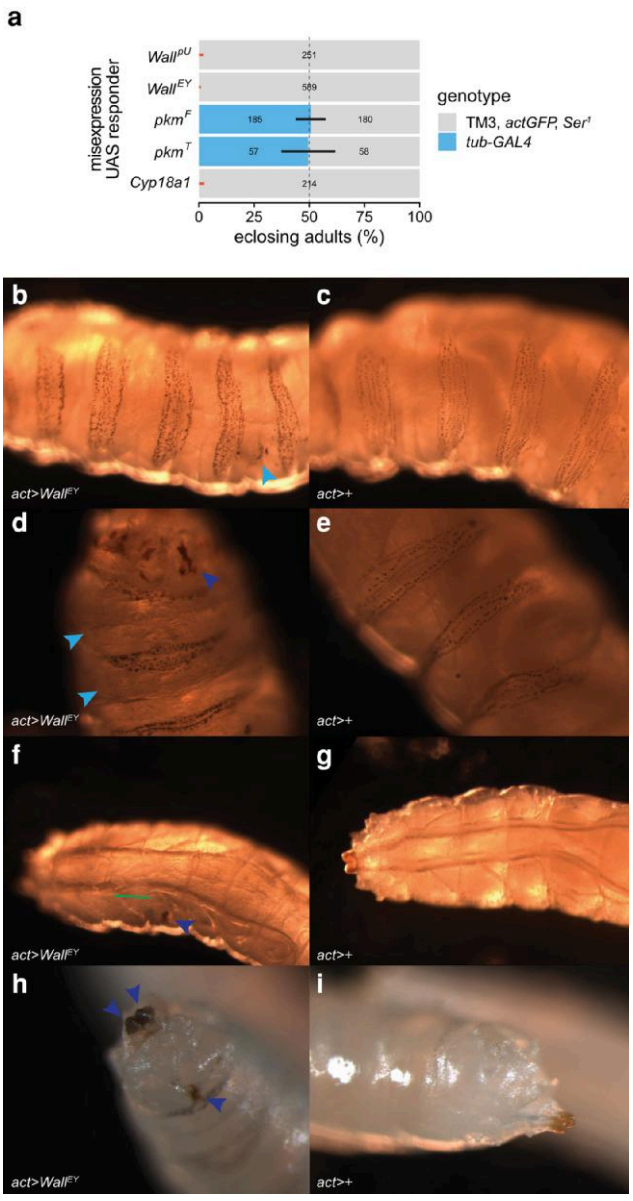

Fig. 3. Ubiquitous misexpression of *Wall*, *pkm*, and *Cyp18a1*. a) Egg-to-adult viability of strong, ubiquitous *Wall*, *pkm*, and *Cyp18a1* misexpression, estimated from the adult genotypic ratios of offspring from crosses between *tub-GAL4*/TM3 *actGFP* Ser^1 females (genotypes in bold) and UAS-responder males at 25°C. UAS-pkm^F expresses the full 635 aa *pkm* ORF, while UAS-pkm^T expresses a truncated 430 aa ORF that does not include the pkm N-terminal disordered region. The dashed line indicates the expected 1:1 genotypic ratio if both genotypes per cross are equally developmentally viable; error bars are 99% confidence intervals (95% CI adjusted for 5 tests) for the proportion of *GAL4*-containing heterozygotes; black and red bars indicate nonsignificant or significant deviations, respectively, from expected genotypic ratios after correction for multiple tests. Numbers on the bars are the number of adults of each genotype (for numbers greater than 0). b–i) Phenotypes in larvae misexpressing UAS-$Wall^{EY}$ with the *act-GAL4* driver (*act* > $Wall^{EY}$; left) compared with wild-type, non-misexpressing larvae (*act*>+; right), at 25°C. b–e) Denticle belt disorganization, including ectopic denticles in between belts (light blue arrowheads) and rectal pad melanization (dark blue arrowheads). (f and g) Fluid-filled section of a tracheal dorsal trunk (green line segment), along with a melanized section of trachea (dark blue arrowhead). (h and i) Melanized posterior spiracles and rectal pad (dark blue arrowheads).

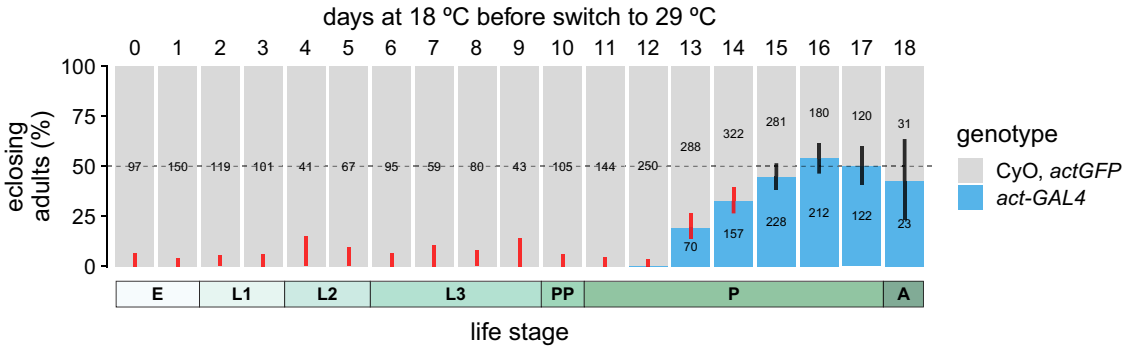

Fig. 4. Delayed onset of ubiquitous misexpression of *Wall* arrests development up until mid-metamorphosis. Top: egg-to-adult viability of *Wall* misexpression with the ubiquitous driver *act-GAL4*, in concert with the UAS-*Wall*^{EY} element and the temperature-sensitive *tub-GAL80*^{ts} construct, which inhibits GAL4 at 18°C but not at 29°C; animals were moved from 18°C to 29°C at 1 of 19 timepoints (top), which began *Wall* misexpression. Viability is estimated from the adult genotypic ratios of offspring from crosses between *act-GAL4*/CyO *actGFP* females and *tub-GAL80*^{ts}; UAS-*Wall*^{EY} males. The dashed line indicates the expected 1:1 genotypic ratio if both genotypes per cross are equally developmentally viable; error bars are 99.7% confidence intervals (95% CI adjusted for 19 tests) for the proportion of *act-GAL4*-containing heterozygotes; black and red bars indicate nonsignificant or significant deviations, respectively, from expected genotypic ratios after correction for multiple tests. Numbers on the bars are the number of adults of each genotype (for numbers greater than 10). Bottom: approximate developmental life stages of *D. melanogaster* at 18°C, showing *Wall*-sensitive (red) and *Wall*-insensitive (black) developmental periods; dashed line indicates region of uncertainty. E, embryo; L1, 1st-instar larva; L3, 2nd-instar larva; L3, 3rd-instar larva; PP, prepupa; P, pupa; A, adult.

which strongly expresses GAL4 in a ubiquitous pattern (*tub-GAL4* was not used because pilot experiments suggested that *tub-GAL80*^{ts} was unable to fully repress its activity). Misexpression of *Wall* caused significant reductions in egg-to-adult viability when delayed 0–14 days into development, but did not significantly affect viability from 15–18 days (at 18° C adult emerge at ~18 days), suggesting that animals become insensitive to *Wall* misexpression around the middle of metamorphosis (Fig. 4).

Tissue-specific misexpression of *Wall* causes developmental arrest distinct from *Cyp18a1*

The developmental arrest phenotype observed upon ubiquitous misexpression of *Wall* is consistent with an EcK function of its encoded protein. To further test this hypothesis, we conducted tissue-specific misexpression crosses to explore if the patterns of developmental arrest produced by *Cyp18a1* misexpression matched that of *Wall* misexpression; a close match would be good evidence that Wall and Cyp18a1 act on the same or similar substrates.

Misexpression of *Wall* was conducted with 2 ubiquitous GAL4 drivers (*tub-GAL4*, used previously, and *da-GAL4*, a weaker driver) and 14 tissue-specific GAL4 drivers (Supplementary Table 1). The positive control UAS-*Cyp18a1* construct produced developmental arrest when misexpressed with all 16 drivers (Fig. 5; Supplementary Table 4). The UAS-*Wall*^{EY} construct produced developmental arrest when misexpressed with 10 drivers, while the UAS-*Wall*^{pU} construct produced very similar results, but with no phenotype with the *ppl-GAL4* driver and generally caused developmental arrest at later life stages (Fig. 5; Supplementary Table 4). Misexpression of UAS-*Wall*^{pU} with *btl-GAL4* and *cg-GAL4* also resulted in a small number of adult escapers (Fig. 5b; Supplementary Table 4). These differences between UAS-*Wall* transgenes are likely due to differences in expression strength: the *EPgy2* element contains 14 copies of UAS in its artificial enhancer region (Bellen *et al.* 2004), while pUASTattB contains only 5 (Bischof *et al.* 2007). However, the broad consistency of the results from both an independent transgene construct and a native locus misexpression construct means these phenotypes can be confidently linked to the ectopic expression of the *Wall* ORF.

Misexpressing UAS-*Wall*^{EY} with the *HR-GAL4* driver resulted in a dramatic phenotype: an extended wandering period during the 3rd larval instar, then defects during pupariation and pupation wherein the puparium was thin and elongated and anterior adult tissue differentiation appeared to occur without head eversion, resulting in dark thoracic (likely from wings) and red eye pigmentation developing internally (Supplementary Fig. S7A–C). This phenotype suggests that *Wall* misexpression with this driver can block epidermal and cuticular development during metamorphosis, but curiously still allows for imaginal discs eversion to take place. The *HR-GAL4* driver expresses GAL4 along the whole length of the midgut, as well as in the Malpighian tubules and the fat body (Chung *et al.* 2007); however, the lack of phenotypes with the enterocyte-specific *mex1-GAL4* driver (Phillips and Thomas 2006) suggests that *Wall* misexpression in these midgut cells does not cause developmental defects. Additionally, given that the fat body drivers *cg-GAL4* and *ppl-GAL4* failed to phenocopy *HR-GAL4*, the crucial tissues might be non-enterocyte midgut cells and/or the Malpighian tubules. Alternatively, *HR-GAL4* may drive at a low (yet sufficient) level in another tissue to produce this phenotype, such as the muscles.

Conspicuously, while the *phm-GAL4* driver, which expresses GAL4 in the prothoracic cells of the ring gland (PG)—the ecdysteroidogenic tissue in larvae (Redfern 1983)—as well as some other tissues such as the wing disc (Casas-Tintó *et al.* 2017)—caused embryonic lethality when misexpressing *Cyp18a1* as expected, it produced no developmental arrest when misexpressing either *Wall* construct (Fig. 5b). This result appears inconsistent with *Wall* encoding a kinase that can act on ecdysteroids present in the PG, although it could be explained by the action of an ecdysteroid-phosphate phosphatase in these cells.

Misexpression of *Wall* with the *c204-GAL4* driver caused larval arrest with the UAS-*Wall*^{EY} construct and arrest during metamorphosis with the UAS-*Wall*^{pU} construct (Fig. 5). The expression pattern of this driver is not well characterized—while it is known to be expressed in the adult ovary (Manseau *et al.* 1997), it may be expressed in other tissues and at other life stages, given it causes embryonic arrest with UAS-*Cyp18a1* and the aforementioned arrest with UAS-*Wall* constructs. Curiously, *elav-GAL4* misexpression of *Wall* caused developmental arrest, while *nSyb-GAL4* misexpression did not, suggesting that misexpression in neurons is not the cause of *elav-GAL4* arrest; the *elav-GAL4* driver, while often considered specific to neurons, expresses in other tissues, such as glia, trachea and the imaginal discs (Berger *et al.* 2007; Casas-Tintó *et al.* 2017), 1 or more of which is likely the cause of the developmental arrest observed here.

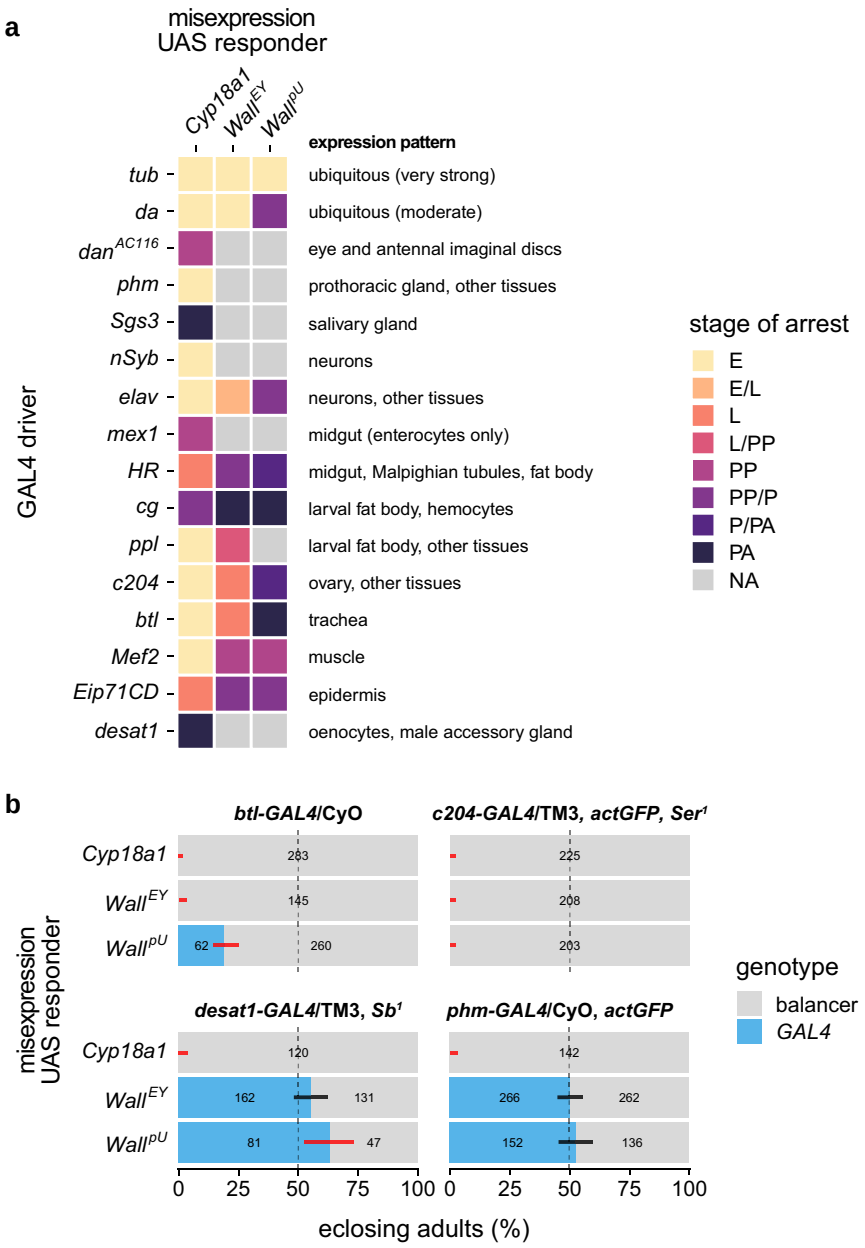

Fig. 5. Tissue-specific misexpression of *Wall* and *Cyp18a1*, using the UAS-*Wall*^{EY}, UAS-*Wall*^{pU}, and UAS-*Cyp18a1* constructs, at 25°C. a) Heat map of qualitative developmental arrest phenotypes for *Wall* and *Cyp18a1* misexpression using 2 ubiquitous GAL4 drivers and 14 tissue-specific GAL4 drivers. E, embryo; L, larva; PP, prepupa; P, pupa; PA, pharate adult; NA, no arrest (successful eclosion). When arrest occurred at more than 1 stage, 2 stages are indicated and separated with a slash. For phenotypic descriptions, see Supplementary Table 4. b) Egg-to-adult viability of *Wall* and *Cyp18a1* misexpression, estimated from the adult genotypic ratios of offspring from crosses between *GAL4*/balancer females (genotypes in bold) and UAS-responder males. The dashed line indicates the expected 1:1 genotypic ratio if both genotypes per cross are equally developmentally viable; error bars are 98.3% confidence intervals (95% CI adjusted for 3 tests) for the proportion of *GAL4*-containing heterozygotes; black and red bars indicate nonsignificant or significant deviations, respectively, from expected genotypic ratios after correction for multiple tests. Numbers on the bars are the number of adults of each genotype (for numbers greater than 0).

Overall, these data demonstrate that *Wall* misexpression in the trachea, muscle, epidermis, or fat body is sufficient to cause developmental arrest, while misexpression in the PG, imaginal discs, salivary gland, neurons, or oenocytes does not cause any obvious phenotype. In addition, combined with the results of the ubiquitous delayed-onset misexpression experiment (Fig. 4), these data suggest that the pharate adult lethality observed through misexpression with some drivers (*cg-GAL4* and *btl-GAL4*) may be due to misexpression of *Wall* during or before early metamorphosis, not during the pharate adult stage itself.

Larval tracheal misexpression of *Wall* causes tracheal defects and food aversion

Misexpression of *Wall* with the trachea-specific *btl-GAL4* driver caused developmental arrest at the larval or pharate adult stages, depending on the UAS-responder construct and the temperature (Fig. 5, Supplementary Table 4). We noticed that 1st- or 2nd-instar *btl* > *Wall*^{EY} larvae raised at 25°C abandoned the food media to crawl up the sides of the vial and died before pupariation, a phenotype that was shared with ubiquitously misexpressing *da* > *Wall*^{EY} larvae that were escaped from embryonic lethality using the *tub-GAL80*^{ts}

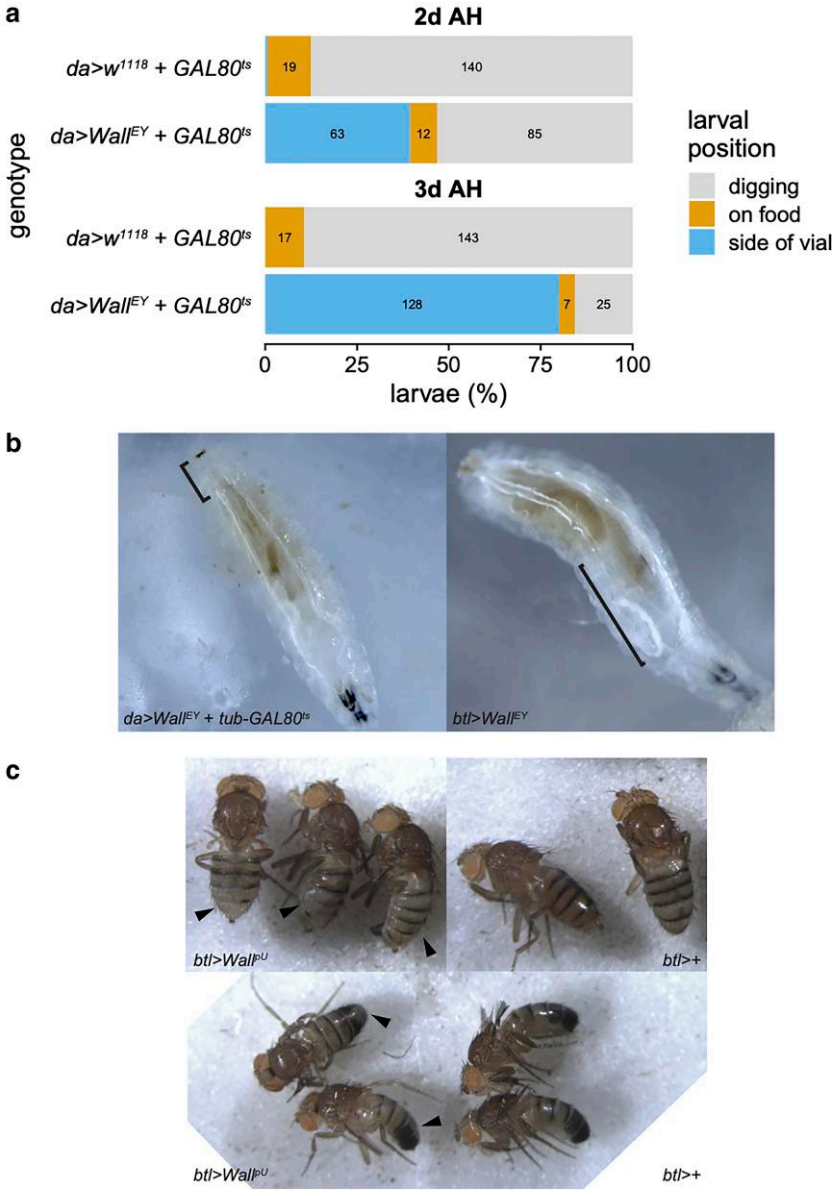

Fig. 6. Misexpression of *Wall* affects tracheal integrity and adult pigmentation. a) Food avoidance assay comparing *da* > w^{1118} + *GAL80*^{ts} and *da* > *Wall*^{EY} + *GAL80*^{ts} larvae 2 days (top) and 3 days (bottom) after hatching (AH). Numbers on the bars are the number of larvae in each position (for numbers greater than 5). b) Photos of larvae misexpressing *Wall* ubiquitously (*da* > *Wall*^{EY} + *tub-GAL80*^{ts}, left) or specially in the trachea (*btl* > *Wall*^{EY}, right) retrieved from food media at 25°C, before food aversion occurred. Black segments indicate sections of tracheal dorsal trunks that are filled with liquid. c) Adult flies (females, top; males, bottom) misexpressing *Wall* in the trachea (*btl* > *Wall*^{pU}, left) or with the *btl-GAL4* driver alone (*btl*>+, right). Arrowheads indicate dorsal abdomen pigmentation defects (areas of lightened pigment compared to the rest of the abdomen). Wings have been removed to expose the dorsal abdomen.

construct and then moved to 29°C, as well as the *act* > *Wall*^{EY} larvae described previously. Quantification of this food-aversion phenotype showed *da* > *Wall*^{EY} larvae were positioned differently within vials compared to non-misexpressing *da* > w^{1118} controls, at both 2 days and 3 days after hatching (both $P < 2.2 \times 10^{-16}$, Fisher's exact test; Fig. 6a). There was also a significant difference in positions between the 2 timepoints for misexpressing larvae ($P = 9.7 \times 10^{-14}$, Fisher's exact test), while there was no significant difference between non-misexpressing larvae ($P = 0.73$, Fisher's exact test), consistent with progression of the misexpression phenotype over time (Fig. 6a). Food aversion is a well-established consequence of hypoxia in both larvae and adult *D. melanogaster* (Vigne and Frelin 2010; Wang *et al.* 2015; Wingen *et al.* 2017)—consistent with this, close examination of *btl* > *Wall*^{EY} and *da* > *Wall*^{EY} larvae revealed defects in tracheal filling (similar to those seen in *act* > *Wall*^{EY} and *c204* > *Wall*^{EY} larvae; Fig. 3f, Supplementary Table 4), with parts of the dorsal trunks often filled with liquid (Fig. 6b), which can cause severe reductions in gas exchange (Parvy *et al.* 2012). Taken together, these data suggest that *Wall* misexpression in trachea causes hypoxia through defects in either tracheal development, maintenance, or integrity. The food-aversion phenotype is also the basis for the gene name *Wallflower* (*Wall*), due to the tendency of the larvae to position themselves on the walls of the vial, rather than in the food with other larvae, an allusion to the "wallflower"? metaphor for social behavior.

Misexpression of *Wall* with the *btl* driver also appears to affect tissues other than the trachea, as we noticed a pigmentation defect on the dorsal abdomen of both male and female *btl* > *Wall*^{pU} adult escapers (Fig. 6c).

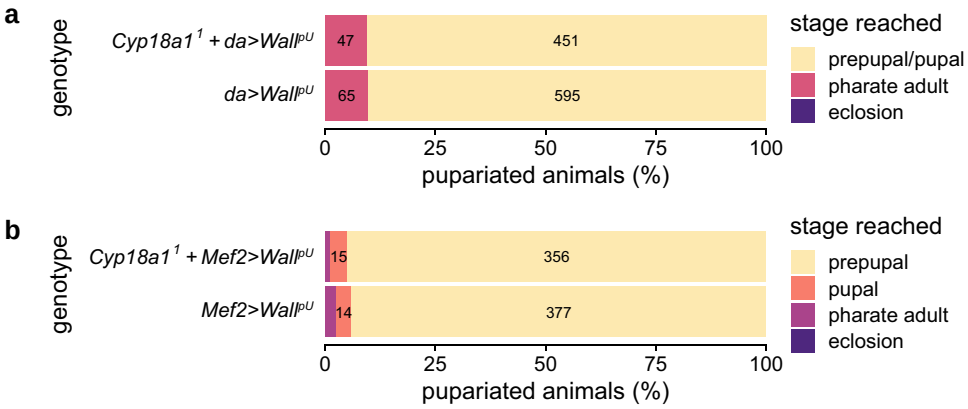

Fig. 7. Tests of hypostasis between $Wall^{pU}$ misexpression and *Cyp18a1*, using a) the moderate, ubiquitous driver *da-GAL4* and b) the muscle-specific driver *Mef2-GAL4*. Genotypes are pooled offspring genotypes from crosses with $Cyp18a1^{1}$/FM7i *actGFP* chrX mothers (25% of offspring are $Cyp18a1^{1}$ hemizygotes) or wild-type chrX mothers (100% of offspring have wild-type *Cyp18a1*). The number of individuals was not quantified before the prepupal stage, so proportions are given as the percentage of pupariated animals per genotype. Numbers on the bars are the number of individuals in each lethal phase category (for numbers greater than 10).

Wall misexpression phenotypes are not hypostatic to *Cyp18a1*

We hypothesized that *Wall* encodes an ecdysteroid 26-kinase, an enzyme that can only act on the products of the ecdysteroid 26-hydroxylase Cyp18a1 (Fig. 1). If this hypothesis is true, *Wall* misexpression should be hypostatic to the wild-type function of *Cyp18a1*—i.e. misexpression of an ecdysteroid 26-kinase (Wall) should not cause developmental defects when the source of 26-hydroxyecdysteroids (Cyp18a1) is not functional. Data indicating hypostasis would be strong genetic evidence of a biochemical interaction between the 2 genes and would support the hypothesis that *Wall* encodes an ecdysteroid 26-kinase. In contrast to $Cyp18a1^{1}$ animals, which largely reach the pharate adult stage but fail to eclose (Rewitz *et al.* 2010), most *da* > $Wall^{pU}$ animals at 25°C arrest development before the differentiation of adult structures (prepupal/pupal arrest; Supplementary Table 4), while most *Mef2* > $Wall^{pU}$ animals arrest development before pupation (prepupal arrest; Supplementary Table 4). We reasoned that if *Wall* misexpression phenotypes were hypostatic to the function of *Cyp18a1*, $Cyp18a1^{1}$ hemizygotes (25% of the offspring of crosses between $Cyp18a1^{1}$/FM7i, *actGFP*; UAS-$Wall^{pU}$ females and GAL4 males) should reach the pharate adult stage instead of earlier developmental arrest due to *Wall* misexpression, increasing the proportion of pharate adult-lethal animals compared to crosses without the $Cyp18a1^{1}$ allele.

There were no significant differences in developmental outcomes between $Cyp18a1^{1}$, *Mef2* > $Wall^{pU}$, and *Mef2* > $Wall^{pU}$ offspring (Fig. 7a; $P = 0.336$, Fisher's exact test), nor between $Cyp18a1^{1}$, *da* > $Wall^{pU}$, and *da* > $Wall^{pU}$ offspring (Fig. 7b; $P = 0.841$, Fisher's exact test). These data indicate that misexpression of *Wall* in $Cyp18a1^{1}$ hemizygotes produces the same developmental arrest phenotypes as misexpression of *Wall* in a wild-type background, strongly suggesting that *Wall* is not hypostatic to *Cyp18a1*, and that *Wall* is unlikely to encode an ecdysteroid 26-kinase.

Pkm mutants are not sensitive to starvation

pkm was found by Chatterjee *et al.* (2014) to be up-regulated in adult female oenocytes upon starvation, which led to the hypothesis that *pkm* plays a role in the metabolic response to starvation, and that *pkm* loss-of-function mutants are more susceptible to starvation. Wet-starvation experiments (Storelli *et al.* 2019) were conducted with virgin male and virgin female flies, the offspring from 3 different crosses: pkm^{4} females and w^{1118} males (yielding pkm^{4}/pkm^{+} females and pkm^{4}/Y males); pkm^{4} females and pkm^{2} males (yielding pkm^{4}/pkm^{2} females and pkm^{4}/Y males); and w^{1118} females and pkm^{2} males (yielding pkm^{2}/pkm^{+} females and pkm^{+}/Y males). For heterozygous female genotypes, median survival in days were 9 (95% CI: 8, 9), 8 (95% CI: 8, 8), and 9 (95% CI: 8, 9) for pkm^{4}/pkm^{2}, pkm^{4}/pkm^{+}, and pkm^{2}/pkm^{+}, respectively, with no significant differences between any pairs of genotypes across entire survival curves (all $P > 0.6$, log-rank test; Supplementary Fig. S8A). For hemizygous male genotypes, median survival in days were 7 (95% CI: 6, 7), 8 (95% CI: 7, 9), and 6 (95% CI: 6, 7) for pkm^{4}/Y (pkm^{2} father), pkm^{4}/Y (w^{1118} father), and pkm^{+}/Y (pkm^{2} father), respectively, with the only significant difference between the pkm^{4}/Y (pkm^{2} father) and pkm^{4}/Y (w^{1118} father) across entire survival curves genotypes ($P = 0.0037$, log-rank test; all other $P > 0.067$; Supplementary Fig. S8B). These data do not support the hypothesis that *pkm* is involved in starvation resistance.

Misexpression of *CG5644*, another strong EcK candidate gene, also causes developmental arrest

As other EcKLs in the *D. melanogaster* genome may also encode EcKs, we screened an additional 13 EcKLs for misexpression phenotypes using preexisting UAS-ORF fly lines and the *tub-GAL4* driver. Six of these genes—*CG31300*, *CG31288*, *CG10560*, *CG10562*, *CG6830*, and *JhI-26*—were previously considered candidate detoxification genes, while the 7 others—*CG10514*, *CG31102*, *CG31087*, *CHKov2*, *CG9259*, *CG14314*, and *CG5644*—were not (Scanlan *et al.* 2020).

Only misexpression of *CG6830* and *CG5644* caused significant developmental arrest before the adult stage (Fig. 8a). The UAS-*CG5644* line was further crossed to the *phm-GAL4* driver at 25°C, resulting in 66 misexpression adults surviving compared to 115 balancer adults (proportion = 0.365, 95% CI: 0.295–0.439, $P = 0.0003$, binomial test), suggesting that PG misexpression of *CG5644* can also disrupt development. These data are consistent with the hypothesis that *CG5644* encodes an ecdysteroid 22-kinase, previously proposed based on 1:1 orthology to *AgEcK2* in *A. gambiae* (Peng *et al.* 2022; Scanlan and Robin 2024). The lack of developmental arrest seen in *tub* > *CG31300* and *tub* > *JhI-26* individuals is consistent with previously published experimental data (Liu *et al.* 2014; Scanlan *et al.* 2022).

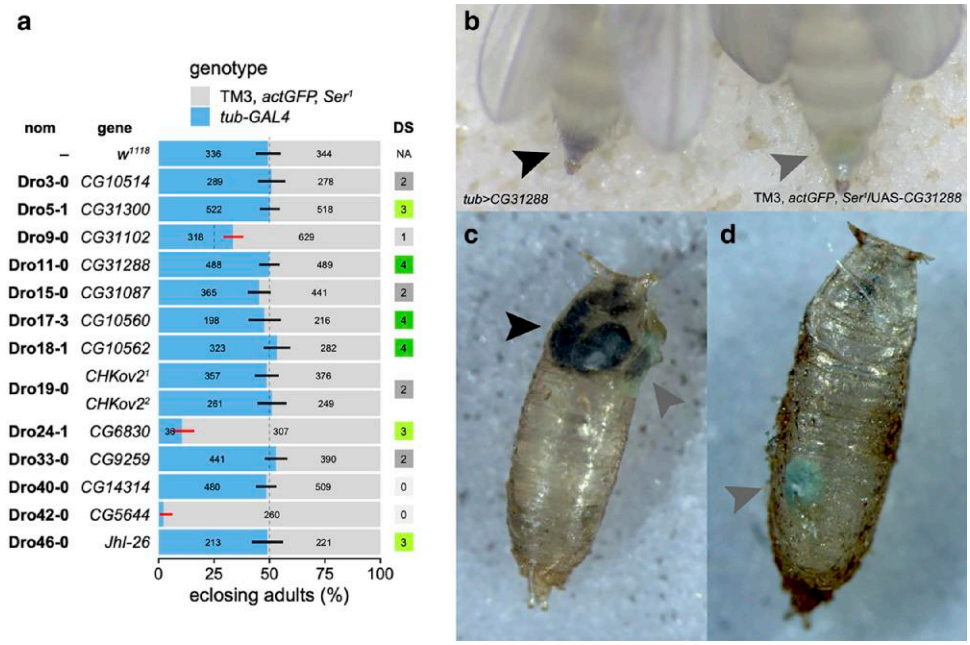

Fig. 8. Misexpression of 13 additional EcKL genes to find candidate EcKs. a) Egg-to-adult viability of the misexpression of 13 EcKLs (and 1 control genotype, w^{1118}), estimated from the adult genotypic ratios of offspring from crosses between *tub-GAL4*/TM3, *actGFP*, Ser^1 females and UAS-responder males at 25°C. The dashed line indicates the expected 1:1 genotypic ratio (or the 1:3 genotypic ratio for CG31102) if both genotypes per cross are equally developmentally viable; error bars are 99.7% confidence intervals (95% CI adjusted for 15 tests) for the proportion of *GAL4*-containing heterozygotes; black and red bars indicate nonsignificant or significant deviations, respectively, from expected genotypic ratios after correction for multiple tests. Numbers on the bars are the number of adults of each genotype (for numbers greater than 6). nom, *Drosophila* EcKL nomenclature (Scanlan *et al.* 2020); DS, detoxification score, where 3 or 4 is considered a candidate detoxification gene (Scanlan *et al.* 2020); NA, not applicable for w^{1118}. b) Meconium of freshly eclosed female flies, visible within the posterior tip of the abdomen before excretion. Black arrowhead, dark meconium of a *tub* > CG31288 fly; gray arrowhead, wild-type (green) meconium of a TM3 *actGFP* Ser^1/UAS-CG31288 fly. c) Meconium deposited on the empty puparium of a fly from the cross between *tub-GAL4*/TM3 *actGFP* Ser^1 and UAS-CG31288. Black arrowhead, dark meconium of a *tub* > CG31288 fly; gray arrowhead, wild-type (green) meconium of a TM3, *actGFP* Ser^1/UAS-CG31288 fly. d) Yellow-green meconium deposited on the empty puparium of a wild-type w^{1118} fly (gray arrowhead).

While misexpression of CG31288 did not appear to affect developmental progression, we noticed a visible phenotype for *tub* > CG31288 adult flies: their meconium was a dark gray, almost black color, compared to the yellow-green of non-misexpressing flies (Fig. 8b–d). This color change was apparent both within the posterior abdomen of recently eclosed flies (Fig. 8b) and when the meconium had been excreted and left on empty puparia (Fig. 8c and d).

Discussion

Here we have performed the first detailed genetic characterization of candidate ecdysteroid kinase (EcK) genes in insects, targeting *Wall* and *pkm*, orthologs of the *B. mori* ecdysteroid 22-kinase gene *BmEc22K*. Despite phenotypic discrepancies between gene disruption methods, we ultimately found no clear evidence that these genes encode EcKs that have essential functions in development or reproduction. Tissue-specific misexpression was also used to detect possible EcK activity, which produced striking developmental disruption phenotypes for *Wall* but not for *pkm*.

The phenotypic differences we observed between our null allele, RNAi knockdown, and somatic CRISPR knockout approaches were unexpected. Broadly, strong RNAi knockdown conditions resulted in developmental arrest for both genes, across independent dsRNA constructs, but homozygous mutant animals (including double mutants) showed no obvious developmental phenotypes and had similar viability to controls (see Supplementary Table 3 for a summary). One explanation is genetic compensation in null mutants that is not trigged during RNAi knockdown (El-Brolosy and Stainier 2017), but knocking down *pkm* in a *pkm* mutant background did not rescue developmental arrest, inconsistent with this hypothesis. The more likely explanation then is that the RNAi knockdown phenotypes were due to off-target effects, which have been well documented in *Drosophila* (Seinen *et al.* 2011). For *Wall*, no phenotypes were detected for both null alleles and somatic CRISPR knockout, however for *pkm*, somatic CRISPR knockout produced a highly penetrant motor coordination defect not seen in null mutant animals. Explanations for this are unclear, but might be linked to CRISPR-Cas9 off-target cleavage or unintended effects on the splicing or transcriptional regulation of *nod*, the fourth intron of which contains *pkm*.

Null alleles are generally considered the gold standard for characterization of gene function. Animals homozygous or hemizygous for null alleles of *Wall*, *pkm*, or both genes appeared indistinguishable from wild-type animals respect to both developmental progression and reproduction, strongly suggesting that these 2 closely related EcKLs do not play important roles in these processes, even redundantly with each other. This is in contrast with *BmEc22K*, another subfamily A EcKL that encodes an ecdysteroid 22-kinase involved in ovary–embryo ecdysteroid recycling (Sonobe *et al.* 2006), and indicates that this function is not conserved in dipteran subfamily A genes. It is possible *Wall* and/or *pkm* null mutants have subtle or environmentally specific phenotypes we were unable to detect in our experiments, although the lack of expression of either gene in reproductive tissues (Leader *et al.* 2018) makes this unlikely for reproductive functions. The lack of strict conservation of the EcKL clades containing *pkm* and *Wall* (referred to as Dip9 and Dip10 in Scanlan and Robin 2024) is consistent with nonessential functions of these genes in *Drosophila* and other dipteran taxa.

Neither null mutants nor misexpression animals for *pkm* displayed any obvious phenotypes, offering no clue as to the gene's native function or enzymatic activity. We hypothesized that *pkm*

is involved in the starvation response in adult flies, based on transcriptomic data from Chatterjee *et al.* (2014), but experiments with null mutants did not show a difference in wet starvation survival compared to control genotypes, for either sex, offering no support for the hypothesis. Using RNAi knockdown with the same dsRNA lines used here, Santana *et al.* (2020) suggested that the Pkm protein controls mRNA and protein abundances of Hsp23 and Hsp26, leading to modulation of synaptogenesis and neural response to stress. However, our results cast doubt on the interpretability of RNAi knockdown of *pkm* and suggest that off-target effects could be responsible for these phenotypes. Confirmation of neural functions of *pkm* could be done with null alleles, which we show here to be viable and therefore could allow the study of subtle neurological phenotypes at any life stage.

Like *pkm*, *Wall* null mutants had no obvious phenotypes. However, misexpression of *Wall* disrupted developmental progression with both ubiquitous and tissue-specific drivers, suggesting that the Wall protein can act on 1 or more developmentally important small molecules. Tissues sensitive to *Wall* misexpression are the trachea, fat body, epidermis, and muscle, while insensitive tissues are the PG, neurons, oenocytes, imaginal discs, and salivary glands. Ubiquitous misexpression of *Wall* caused developmental arrest at all life stages, except past the midpoint of metamorphosis, after pupal–adult apolysis has occurred (Bainbridge and Bownes 1981). These data suggest that the substrate(s) of Wall could have essential signaling functions in trachea, fat body, epidermis, and muscle across *D. melanogaster* development. However, we believe it is unlikely these substrates are E and/or 20E, as: (1) embryonic *Wall* misexpression did not phenocopy the "Halloween"? phenotype like *Cyp18a1* (Rewitz *et al.* 2010); (2) *Wall* phenotypes were specific to certain tissues, while *Cyp18a1* misexpression reliably caused developmental arrest in tissues known to rely on 20E signaling; and (3) *Wall* misexpression in the PG, the larval source of E, did not produce developmental arrest, unlike *Cyp18a1*. Curiously, however, a recent paper reports that the dorsal internal oblique muscles (DIOMs) are the source of the mid-pupal pulse of 20E (Zhang *et al.* 2024). Metamorphic defects seen upon pan-muscular *Wall* misexpression could be consistent with interfering with ecdysteroid signaling in DIOMs, although these generally occurred before the middle of metamorphosis (Fig. 5a).

If Wall can indeed phosphorylate E and/or 20E, the tissue-specific phenotypes of Wall misexpression may have alternative explanations. One such explanation could be the presence of tissue-specific phosphatases that hydrolyze ecdysteroid-phosphates back to active hormones. Another explanation could be tissue-specific post-transcriptional or post-translational regulation of *Wall* that reduces the level of active enzyme and dampens or eliminates the effects of misexpression in certain cell types.

An ecdysteroid 26-kinase is known to be active in the S2 cell line (Guittard *et al.* 2011), which we hypothesized could be encoded by *Wall* due to transcriptional similarities to the ecdysteroid 26-hydroxylase/carboxylase gene *Cyp18a1*. However, this hypothesis was not supported by epistasis experiments, which found that the severity of *Wall* misexpression phenotypes was not reduced in a *Cyp18a1* mutant background, suggesting that *Wall*-induced developmental defects are to not due to phosphorylation of 26-hydroxylated ecdysteroids produced by Cyp18a1. Alternative candidates for encoding this ecdysteroid 26-kinase are *CG2004*, *CG31975*, and *JhI-26*, which are all basally expressed in S2 cells to appreciable degrees (Supplementary Fig. 9).

Plausible, alternative ecdysteroid substrates for Wall are 3-dehydroecdysteroids and 3-epiecdysteroids, which are produced in the fat body and epidermis of larvae (Sommé-Martin *et al.* 1988a, 1988b) and may have signaling functions in *D. melanogaster* (Sommé-Martin *et al.* 1990; Baker *et al.* 2003). The physiological functions of these modified ecdysteroids are still unclear in *D. melanogaster*, but intriguingly, 3-dehydro-20E was recently found to modulate female reproductive physiology in the mosquito *A. gambiae* (Peng *et al.* 2022). Additionally, Cavigliasso *et al.* (2024) recently suggested that *fezzik* (*fiz*) encodes an ecdysteroid oxidase that adaptively modulates larval growth rate under malnutrition in *D. melanogaster*. If oxidized ecdysteroids control larval development, they would be good candidate substrates for Wall. Other possible substrates could be produced by Cyp301a1, Cyp303a1, and Spidey, developmentally important yet biochemically uncharacterized enzymes with various links to ecdysteroid metabolism (Sztal *et al.* 2012; Chiang *et al.* 2016; Wu *et al.* 2019).

The phenotypes associated with *Wall* misexpression might not necessarily reflect the gene's wild-type function, as the enzyme may be acting promiscuously on substrates that it rarely or never encounters in non-transgenic animals. However, if they are attributable to native substrates, these misexpression phenotypes might still be exposing novel hormonal pathways that underpin important developmental processes. Such native substrates would clearly be involved in tracheal integrity, cuticle and epidermal development, and functions of the fat body and muscles during metamorphosis. These are all known to be regulated by ecdysteroid signaling (Zachary and Hoffmann 1980; Bond *et al.* 2010; Chanut-Delalande *et al.* 2014; Buhler *et al.* 2018), but links to signaling genes and proteins that have been associated with more than 1 of the developmental defects seen in *Wall*-misexpressing animals could offer mechanistic clues. These include: the scavenger receptor Dsp, which is involved in both tracheal integrity and adult pigmentation (Dembeck *et al.* 2015; Wingen *et al.* 2017); *Megf8*, which is involved in tracheal integrity and denticle belt development (Lloyd *et al.* 2018); and Svb, which has roles in tracheal and denticle belt development (Chanut-Delalande *et al.* 2006, 2014). Intriguingly, Svb also acts in the adult midgut to coordinate stem cell behavior under the control of EcR (Al Hayek et al. 2021), which is a major site of native *Wall* expression (Leader *et al.* 2018). Ultimately, biochemical characterization of the purified Wall protein is needed to fully understand its signaling interactions upon misexpression.

The results of this study leave as open questions the identities of the ecdysteroid 2-, 3-, 22-, and 26-kinases in *D. melanogaster*. However, data from our misexpression experiments are consistent with *CG5644* encoding an EcK, especially the developmental arrest seen upon PG-specific misexpression of this gene. Curiously, developmental arrest upon PG misexpression was only partially penetrant, raising the possibility that an ecdysteroid-phosphate phosphatase is present in this tissue. Our previous phylogenetic analyses of the EcKL gene family determined that *CG5644* is a 1:1 ortholog of *AgEcK2*, which encodes an ecdysteroid 22-kinase in *A. gambiae* (Peng *et al.* 2022; Scanlan and Robin 2024). While *CG5644* is predominantly expressed in the adult nervous system (Leader *et al.* 2018), it also appears expressed in the migratory border cells in the ovary (Borghese *et al.* 2006), which might make it responsible for the presence of E 22-phosphate in this tissue (Pis *et al.* 1995; Grau *et al.* 1995). Reverse genetics experiments like those conducted here for *Wall* and *pkm*, as well as biochemical characterization, might uncover the functions of both *CG5644* and ecdysteroid 22-phosphates in *D. melanogaster* development, reproduction, and physiology.

Overall, we here provide the first in-depth functional genetic characterization of candidate EcK genes in insects, focusing on the *BmEc22K* orthologs *Wall* and *pkm* in *D. melanogaster*. While neither gene is essential for reproduction and development, multiple lines of evidence are consistent with Wall being able to inactivate

1 or more signaling molecules essential for development. Whether these molecules are ecdysteroids or other hormones is currently unclear. This work is suggestive of unknown complexity in tissue-specific hormonal signaling in *D. melanogaster* and paves the way for further characterization of the likely ecdysteroid 22-kinase gene CG5644. This work also serves to highlight the possible phenotypic inconsistencies that may arise between functional genetic methodologies and reinforces the importance of multiple, complementary gene disruption approaches when characterizing genes of unknown function.

Data availability

Plasmids are available upon request. Fly strains that are not available in stock centers are available upon request. The authors affirm that all data necessary for confirming the conclusions of the article are present within the article, figures, tables, and supplementary material.

Supplemental material available at G3 online.

Acknowledgments

The authors would like to thank Simon Bullock for the pCFD6 plasmid, *BangloreFly at The National Centre for Biological Services*, the Drosophila Genomics Resource Center (NIH 2P40OD010949) for the UAS-ORF plasmids, and Philip Batterham, Michael Murray, Michael O'Connor, and the Bloomington Drosophila Stock Center (NIH P40OD018537) for *Drosophila* stocks. Information available at FlyBase (NIH U41HG000739) was also used extensively during this study.

Funding

The research was funded through internal funding schemes from the University of Melbourne and by an Australian Government stipend to JLS.

Conflicts of interest

The author(s) declare no conflicts of interest.

Literature cited

Al Hayek S, Alsawadi A, Kambris Z, Boquete J-P, Bohère J, Immarigeon C, Ronsin B, Plaza S, Lemaitre B, Payre F, *et al.* 2021. Steroid-dependent switch of OvoL/Shavenbaby controls self-renewal versus differentiation of intestinal stem cells. EMBO J. 40(4):e104347. doi:10.15252/embj.2019104347.

Bainbridge SP, Bownes M. 1981. Staging the metamorphosis of *Drosophila melanogaster*. J Embryol Exp Morphol. 66:57–80.

Baker KD, Shewchuk LM, Kozlova T, Makishima M, Hassell A, Wisely B, Caravella JA, Lambert MH, Reinking JL, Krause H, *et al.* 2003. The Drosophila orphan nuclear receptor DHR38 mediates an atypical ecdysteroid signaling pathway. Cell. 113(6):731–742. doi:10.1016/s0092-8674(03)00420-3.

Baker KD, Warren JT, Thummel CS, Gilbert LI, Mangelsdorf DJ. 2000. Transcriptional activation of the Drosophila ecdysone receptor by insect and plant ecdysteroids. Insect Biochem Mol Biol. 30(11):1037–1043. doi:10.1016/s0965-1748(00)00075-8.

Beckstead RB, Lam G, Thummel CS. 2007. Specific transcriptional responses to juvenile hormone and ecdysone in Drosophila. Insect Biochem Mol Biol. 37(6):570–578. doi:10.1016/j.ibmb.2007.03.001.

Bellen HJ, Levis RW, Liao G, He Y, Carlson JW, Tsang G, Evans-Holm M, Hiesinger PR, Schulze KL, Rubin GM, *et al.* 2004. The BDGP gene disruption project: single transposon insertions associated with 40% of Drosophila genes. Genetics. 167(2):761–781. doi:10.1534/genetics.104.026427.

Berger C, Renner S, Lüer K, Technau GM. 2007. The commonly used marker ELAV is transiently expressed in neuroblasts and glial cells in the Drosophila embryonic CNS. Dev Dyn. 236(12):3562–3568. doi:10.1002/dvdy.21372.

Beydon P, Girault J-P, Lafont R. 1987. Ecdysone metabolism in Pieris brassicae during the feeding last larval instar. Arch Insect Biochem Physiol. 4(2):139–149. doi:10.1002/arch.940040207.

Bischof J, Björklund M, Furger E, Schertel C, Taipale J, Basler K. 2013. A versatile platform for creating a comprehensive UAS-ORFeome library in Drosophila. Development. 140(11):2434–2442. doi:10.1242/dev.088757.

Bischof J, Maeda RK, Hediger M, Karch F, Basler K. 2007. An optimized transgenesis system for Drosophila using germ-line-specific phiC31 integrases. Proc Natl Acad Sci U S A. 104(9):3312–3317. doi:10.1073/pnas.0611511104.

Bond ND, Hoshizaki DK, Gibbs AG. 2010. The role of 20-hydroxyecdysone signaling in Drosophila pupal metabolism. Comparative Biochemistry and Physiology a-Molecular & Integrative Physiology. 157(4):398–404. doi:10.1016/j.cbpa.2010.08.025.

Borghese L, Fletcher G, Mathieu J, Atzberger A, Eades WC, Cagan RL, Rørth P. 2006. Systematic analysis of the transcriptional switch inducing migration of border cells. Dev Cell. 10(4):497–508. doi:10.1016/j.devcel.2006.02.004.

Buhler K, Clements J, Winant M, Bolckmans L, Vulsteke V, Callaerts P. 2018. Growth control through regulation of insulin signalling by nutrition-activated steroid hormone in Drosophila. Development. 145:dev165654. doi:10.1242/dev.165654.

Casas-Tintó S, Arnés M, Ferrús A. 2017. Drosophila enhancer-Gal4 lines show ectopic expression during development. R Soc Open Sci. 4(3):170039. doi:10.1098/rsos.170039.

Cavigliasso F, Savitsky M, Koval A, Erkosar B, Savary L, Gallart-Ayala H, Ivanisevic J, Katanaev VL, Kawecki TJ. 2024. Cis-regulatory polymorphism at *fiz* ecdysone oxidase contributes to polygenic evolutionary response to malnutrition in *Drosophila*. PLoS Genet. 20(3):e1011204. doi:10.1371/journal.pgen.1011204.

Chanut-Delalande H, Fernandes I, Roch F, Payre F, Plaza S. 2006. Shavenbaby couples patterning to epidermal cell shape control. PLoS Biol. 4(9):e290. doi:10.1371/journal.pbio.0040290.

Chanut-Delalande H, Hashimoto Y, Pelissier-Monier A, Spokony R, Dib A, Kondo T, Bohère J, Niimi K, Latapie Y, Inagaki S, *et al.* 2014. Pri peptides are mediators of ecdysone for the temporal control of development. Nat Cell Biol. 16:1035. doi:10.1038/ncb3052.

Chatterjee D, Katewa SD, Qi Y, Jackson SA, Kapahi P, Jasper H, 2014. Control of metabolic adaptation to fasting by dILP6-induced insulin signaling in Drosophila oenocytes. Proc Natl Acad Sci U S A. 111(50):17959–17964. doi:10.1073/pnas.1409241111.

Chen J-H, Webb TJ, Powls R, Rees HH. 1996. Purification and characterisation of haemolymph 3-dehydroecdysone 3β-reductase in relation to ecdysteroid biosynthesis in the cotton leafworm *Spodoptera littoralis*. Eur J Biochem. 242(2):394–401. doi:10.1111/j.1432-1033.1996.0394r.x.

Chiang YN, Tan KJ, Chung H, Lavrynenko O, Shevchenko A, Yew JY. 2016. Steroid hormone signaling is essential for pheromone production and oenocyte survival. PLoS Genet. 12(6):e1006126. doi:10.1371/journal.pgen.1006126.

Chung H, Bogwitz MR, McCart C, Andrianopoulos A, Ffrench-Constant RH, Batterham P, Daborn PJ. 2007. Cis-regulatory elements in the Accord retrotransposon result in tissue-specific expression of the

Drosophila melanogaster insecticide resistance gene Cyp6g1. Genetics. 175(3):1071–1077. doi:10.1534/genetics.106.066597.

Crocker KC, Hunter MD. 2018. Social density, but not sex ratio, drives ecdysteroid hormone provisioning to eggs by female house crickets (*Acheta domesticus*). Ecol Evol. 8(20):10257–10265. doi:10.1002/ece3.4502.

Davies L, Anderson IP, Turner PC, Shirras AD, Rees HH, Rigden DJ. 2007. An unsuspected ecdysteroid/steroid phosphatase activity in the key T-cell regulator, Sts-1: surprising relationship to insect ecdysteroid phosphate phosphatase. Proteins: Struct. Funct. Bioinf. 67(3):720–731. doi:10.1002/prot.21357.

Dembeck LM, Huang W, Magwire MM, Lawrence F, Lyman RF, Mackay TFC. 2015. Genetic architecture of abdominal pigmentation in *Drosophila melanogaster*. PLoS Genet. 11(5):e1005163. doi:10.1371/journal.pgen.1005163.

Dietzl G, Chen D, Schnorrer F, Su K-C, Barinova Y, Fellner M, Gasser B, Kinsey K, Oppel S, Scheiblauer S, *et al.* 2007. A genome-wide transgenic RNAi library for conditional gene inactivation in Drosophila. Nature. 448(7150):151–156. doi:10.1038/nature05954.

Duffy JB. 2002. GAL4 system in drosophila: a fly geneticist's Swiss army knife. Genesis. 34(1–2):1–15. doi:10.1002/gene.10150.

El-Brolosy MA, Kontarakis Z, Rossi A, Kuenne C, Günther S, Fukuda N, Kikhi K, Boezio GLM, Takacs CM, Lai S-L, *et al.* 2019. Genetic compensation triggered by mutant mRNA degradation. Nature. 568(7751):193–197. doi:10.1038/s41586-019-1064-z.

El-Brolosy MA, Stainier DYR. 2017. Genetic compensation: a phenomenon in search of mechanisms. PLoS Genet. 13(7):e1006780. doi:10.1371/journal.pgen.1006780.

Feldlaufer MF, Svoboda JA, Thompson MJ, Wilzer KR. 1988. Fate of maternally-acquired ecdysteroids in unfertilized eggs of *Manduca sexta*. Insect Biochem. 18(2):219–221. doi:10.1016/0020-1790(88)90027-3.

Fortier E, Belote JM. 2000. Temperature-dependent gene silencing by an expressed inverted repeat in Drosophila. Genesis. 26(4):240–244. doi:10.1002/(sici)1526-968x(200004)26:4<240::aid-gene40>3.0.co; 2-p.

Gauhar Z, Sun LV, Hua S, Mason CE, Fuchs F, Li T-R, Boutros M, White KP. 2009. Genomic mapping of binding regions for the Ecdysone receptor protein complex. Genome Res. 19(6):1006–1013. doi:10.1101/gr.081349.108.

Gibson JM, Isaac RE, Dinan LN, Rees HH. 1984. Metabolism of [3H]-ecdysone in *Schistocerca gregaria*; formation of ecdysteroid acids together with free and phosphorylated ecdysteroid acetates. Arch Insect Biochem Physiol. 1(4):385–407. doi:10.1002/arch.940010409.

Gramates LS, Agapite J, Attrill H, Calvi BR, Crosby MA, Dos Santos G, Goodman JL, Goutte-Gattat D, Jenkins VK, Kaufman T, *et al.* 2022. FlyBase: a guided tour of highlighted features. Genetics. 220(4):iyac035. doi:10.1093/genetics/iyac035.

Grau V, Pis J, Lafont R. 1995. Ovary-specific interaction of ecdysone 22-phosphate with proteins in adult *Drosophila melanogaster* (Diptera: Drosophilidae). Eur J Entomol. 92:189–189.

Graveley BR, Brooks AN, Carlson JW, Duff MO, Landolin JM, Yang L, Artieri CG, van Baren MJ, Boley N, Booth BW, *et al.* 2011. The developmental transcriptome of *Drosophila melanogaster*. Nature. 471(7339):473–479. doi:10.1038/nature09715.

Guittard E, Blais C, Maria A, Parvy J-P, Pasricha S, Lumb C, Lafont R, Daborn PJ, Dauphin-Villemant C. 2011. CYP18A1, a key enzyme of Drosophila steroid hormone inactivation, is essential for metamorphosis. Dev Biol. 349(1):35–45. doi:10.1016/j.ydbio.2010.09.023.

Guruharsha KG, Rual J-F, Zhai B, Mintseris J, Vaidya P, Vaidya N, Beekman C, Wong C, Rhee DY, Cenaj O, *et al.* 2011. A protein complex network of *Drosophila melanogaster*. Cell. 147(3):690–703. doi:10.1016/j.cell.2011.08.047.

Hilton JP. 2004. Isolation and Characterization of Ecdysteroid Phosphotransferases. University of Liverpool.

Hoffmann KH, Bulenda D, Thiry E, Schmid E. 1985. Apolar ecdysteroid esters in adult female crickets, *Gryllus bimaculatus*. Life Sci. 37(2):185–192. doi:10.1016/0024-3205(85)90422-9.

Isaac RE, Rose ME, Rees HH, Goodwin TW. 1983. Identification of the 22-phosphate esters of ecdysone, 2-deoxyecdysone, 20-hydroxyecdysone and 2-deoxy-20-hydroxyecdysone from newly laid eggs of the desert locust, *Schistocerca gregaria*. Biochem J. 213(2):533–541. doi:10.1042/bj2130533.

Isaac RE, Sweeney FP, Rees HH. 1983. Enzymic hydrolysis of ecdysteroid phosphate during embryogenesis in the desert locust (*Schistocerca gregaria*). Biochim Biophys Acta. 50:340.

Ishimoto H, Wang Z, Rao Y, Wu C-F, Kitamoto T. 2013. A novel role for ecdysone in Drosophila conditioned behavior: linking GPCR-mediated non-canonical steroid action to cAMP signaling in the adult brain. PLoS Genet. 9(10):e1003843. doi:10.1371/journal.pgen.1003843.

Jang T, Lee KP. 2015. The genetic basis for mating-induced sex differences in starvation resistance in *Drosophila melanogaster*. J Insect Physiol. 82:56–65. doi:10.1016/j.jinsphys.2015.09.002.

Kannangara JR, Mirth CK, Warr CG. 2021. Regulation of ecdysone production in Drosophila by neuropeptides and peptide hormones. Open Biol. 11(2):200373. doi:10.1098/rsob.200373.

Kaplanis JN, Robbins WE, Thompson MJ, Dutky SR. 1973. 26-Hydroxyecdysone: new insect molting hormone from the egg of the tobacco hornworm. Science. 180(4083):307–308. doi:10.1126/science.180.4083.307.

Lafont R, Dauphin-Villemant C, Warren JT, Rees H. 2012. Ecdysteroid chemistry and biochemistry. In: Insect Endocrinology. Gilbert, LI, editor. Academic Press: San Diego pp. 106–176. doi: 10.1016/B978-0-12-384749-2.10004-4.

Lagueux M, Hoffmann JA, Goltzené F, Kappler C, Tsoupras G, Hetru C, Luu B. 1984. Ecdysteroids in ovaries and embryos of *Locusta migratoria*. In: Proceedings in Life Sciences. Biosynthesis, Metabolism and Mode of Action of Invertebrate Hormones Vol. 283 Springer Berlin Heidelberg pp. 168–180. doi: 10.1007/978-3-642-69922-1_18.

Leader DP, Krause SA, Pandit A, Davies SA, Dow JAT. 2018. FlyAtlas 2: a new version of the *Drosophila melanogaster* expression atlas with RNA-Seq, miRNA-Seq and sex-specific data. Nucleic Acids Res. 46(D1):D809–D815. doi:10.1093/nar/gkx976.

Li Z, Ge X, Ling L, Zeng B, Xu J, Aslam AFM, You L, Palli SR, Huang Y, Tan A. 2014. CYP18A1 regulates tissue-specific steroid hormone inactivation in *Bombyx mori*. Insect Biochem Mol Biol. 54:33–41. doi:10.1016/j.ibmb.2014.08.007.

Liu C, Wang J-L, Zheng Y, Xiong E-J, Li J-J, Yuan L-L, Yu X-Q, Wang Y-F. 2014. Wolbachia-induced paternal defect in Drosophila is likely by interaction with the juvenile hormone pathway. Insect Biochem Mol Biol. 49:49–58. doi:10.1016/j.ibmb.2014.03.014.

Lloyd DL, Toegel M, Fulga TA, Wilkie AOM. 2018. The Drosophila homologue of MEGF8 is essential for early development. Sci Rep. 8(1):1–10. doi:10.1038/s41598-018-27076-y.

Lozano R, Thompson MJ, Svoboda JA, Lusby WR. 1989. Profiles of free and conjugated ecdysteroids and ecdysteroid acids during pupal–adult development of *Manduca sexta*. Arch Insect Biochem Physiol. 12(1):63–74. doi:10.1002/arch.940120106.

Makka T, Seino A, Tomita S, Fujiwara H, Sonobe H. 2002. A possible role of 20-hydroxyecdysone in embryonic development of the silkworm *Bombyx mori*. Arch Insect Biochem Physiol. 51(3):111–120. doi:10.1002/arch.10055.

Manseau L, Baradaran A, Brower D, Budhu A, Elefant F, Phan H, Philp AV, Yang M, Glover D, Kaiser K, *et al.* 1997. GAL4 enhancer traps

expressed in the embryo, larval brain, imaginal discs, and ovary of Drosophila. Dev Dyn. 209(3):310–322. doi:10.1002/(sici)1097-0177(199707)209:3<310::aid-aja6>3.0.co; 2-l.

Maróy P, Kaufmann G, Dübendorfer A. 1988. Embryonic ecdysteroids of *Drosophila melanogaster*. J Insect Physiol. 34(7):633–637. doi:10.1016/0022-1910(88)90071-6.

Matsushima D, Kasahara R, Matsuno K, Aoki F, Suzuki MG. 2019. Involvement of ecdysone signaling in the expression of the doublesex gene during embryonic development in the silkworm, *Bombyx mori*. Sex Dev. 13(3):151–163. doi:10.1159/000502361.

Mazina MY, Nikolenko JV, Fursova NA, Nedil'ko PN, Krasnov AN, Vorobyeva NE. 2015. Early-late genes of the ecdysone cascade as models for transcriptional studies. Cell Cycle. 14(22):3593–3601. doi:10.1080/15384101.2015.1100772.

Modde J-F, Lafont R, Hoffmann JA. 1984. Ecdysone metabolism in *Locusta migratoria* larvae and adults. Int J Invert Reproduct Dev. 7(3):161–183. doi:10.1080/01688170.1984.10510087.

Ohtaki T. 1981. Ecdysteroid metabolism in insects. Integr Comp Biol. 21:727–731. doi:10.1093/icb/21.3.727.

Ono H. 2014. Ecdysone differentially regulates metamorphic timing relative to 20-hydroxyecdysone by antagonizing juvenile hormone in *Drosophila melanogaster*. Dev Biol. 391(1):32–42. doi:10.1016/j.ydbio.2014.04.004.

Ou Q, Zeng J, Yamanaka N, Brakken-Thal C, O'Connor MB, King-Jones K, 2016. The insect prothoracic gland as a model for steroid hormone biosynthesis and regulation. Cell Rep. 16(1):247–262. doi:10.1016/j.celrep.2016.05.053.

Öztürk-Çolak A, Marygold SJ, Antonazzo G, Attrill H, Goutte-Gattat D, Jenkins VK, Matthews BB, Millburn G, Dos Santos G, Tabone CJ. 2024. FlyBase: updates to the Drosophila genes and genomes database. Genetics. 227(1):iyad211. doi:10.1093/genetics/iyad211.

Parvy J-P, Napal L, Rubin T, Poidevin M, Perrin L, Wicker-Thomas C, Montagne J. 2012. *Drosophila melanogaster* acetyl-CoA-carboxylase sustains a fatty acid–dependent remote signal to waterproof the respiratory system. PLoS Genet. 8(8):e1002925. doi:10.1371/journal.pgen.1002925.

Peng D, Kakani EG, Mameli E, Vidoudez C, Mitchell SN, Merrihew GE, MacCoss MJ, Adams K, Rinvee TA, Shaw WR, *et al.* 2022. A male steroid controls female sexual behaviour in the malaria mosquito. Nature. 608(7921):93–97. doi:10.1038/s41586-022-04908-6.

Phillips MD, Thomas GH. 2006. Brush border spectrin is required for early endosome recycling in Drosophila. J Cell Sci. 119(7):1361–1370. doi:10.1242/jcs.02839.

Pis J, Girault JP, Grau V, Lafont R. 1995. Analysis of ecdysteroid conjugates: chromatographic characterization of sulfates, phosphates and glucosides. Eur J Entomol. 92:41–50.

Redfern CPF. 1983. Ecdysteroid synthesis by the ring gland of *Drosophila melanogaster* during late-larval, prepupal and pupal development. J Insect Physiol. 29(1):65–71. doi:10.1016/0022-1910(83)90107-5.

Rewitz KF, O'Connor MB, Gilbert LI. 2007. Molecular evolution of the insect Halloween family of cytochrome P450s: phylogeny, gene organization and functional conservation. Insect Biochem Mol Biol. 37(8):741–753. doi:10.1016/j.ibmb.2007.02.012.

Rewitz KF, Rybczynski R, Warren JT, Gilbert LI. 2006. The Halloween genes code for cytochrome P450 enzymes mediating synthesis of the insect moulting hormone. Biochem Soc Trans. 34(6):1256–1260. doi:10.1042/bst0341256.

Rewitz KF, Yamanaka N, O'Connor MB. 2010. Steroid hormone inactivation is required during the juvenile–adult transition in Drosophila. Dev Cell. 19(6):895–902. doi:10.1016/j.devcel.2010.10.021.

Riddiford LM. 1993. Hormones and Drosophila development. In: Bate M, Martinez-Arias A, editors. The Development of Drosophila melanogaster. Cold Spring Harbor Laboratory Press. p. 899–9392.

Ruaud A-F, Lam G, Thummel CS. 2010. The Drosophila nuclear receptors DHR3 and betaFTZ-F1 control overlapping developmental responses in late embryos. Development. 137(1):123–131. doi:10.1242/dev.042036.

Sakurai S, Warren JT, Gilbert LI. 1989. Mediation of ecdysone synthesis in *Manduca sexta* by a hemolymph enzyme. Arch Insect Biochem Physiol. 10(3):179–197. doi:10.1002/arch.940100303.

Santana E, Reyes T de L, Casas-Tintó S. 2020. Small heat shock proteins determine synapse number and neuronal activity during development. PLoS One. 15(5):e0233231. doi:10.1371/journal.pone.0233231.

Scanlan JL, Battlay P, Robin C. 2022. Ecdysteroid kinase-like (EcKL) paralogs confer developmental tolerance to caffeine in *Drosophila melanogaster*. Curr Res Insect Sci. 2:100030. doi:10.1016/j.cris.2022.100030.

Scanlan JL, Gledhill-Smith RS, Battlay P, Robin C. 2020. Genomic and transcriptomic analyses in Drosophila suggest that the ecdysteroid kinase-like (EcKL) gene family encodes the 'detoxification-by-phosphorylation'enzymes of insects. Insect Biochem Mol Biol. 123:103429. doi:10.1016/j.ibmb.2020.103429.

Scanlan JL, Robin C. 2024. Phylogenomics of the ecdysteroid kinase-like (EcKL) gene family in insects highlights roles in both steroid hormone metabolism and detoxification. Genome Biol Evol. 16(2):evae019. doi:10.1093/gbe/evae019.

Scanlan JL, Robin C, Mirth CK. 2023. Rethinking the ecdysteroid source during *Drosophila* pupal–adult development. Insect Biochem Mol Biol. 152:103891. doi:10.1016/j.ibmb.2022.103891.

Seinen E, Burgerhof JGM, Jansen RC, Sibon OCM. 2011. RNAi-induced off-target effects in *Drosophila melanogaster*: frequencies and solutions. Brief Funct Genomics. 10(4):206–214. doi:10.1093/bfgp/elr017.

Sommé-Martin G, Colardeau J, Beydon P, Blais C, Lepesant JA, Lafont R. 1990. P1 gene expression in Drosophila larval fat body: induction by various ecdysteroids. Arch Insect Biochem Physiol. 15(1):43–56. doi:10.1002/arch.940150105.

Sommé-Martin G, Colardeau J, Lafont R. 1988a. Conversion of ecdysone and 20-hydroxyecdysone into 3-dehydroecdysteroids is a major pathway in third instar *Drosophila melanogaster* larvae. Insect Biochem. 18(7):729–734. doi:10.1016/0020-1790(88)90082-0.

Sommé-Martin G, Colardeau J, Lafont R. 1988b. Metabolism and biosynthesis of ecdysteroids in the Drosophila development mutant ecd1. Insect Biochem. 18(7):735–742. doi:10.1016/0020-1790(88)90083-2.

Sonobe H, Ito Y. 2009. Phosphoconjugation and dephosphorylation reactions of steroid hormone in insects. Mol Cell Endocrinol. 307(1–2):25–35. doi:10.1016/j.mce.2009.03.017.

Sonobe H, Ohira T, Ieki K, Maeda S, Ito Y, Ajimura M, Mita K, Matsumoto H, Wilder MN. 2006. Purification, kinetic characterization, and molecular cloning of a novel enzyme, ecdysteroid 22-kinase. J Biol Chem. 281(40):29513–29524. doi:10.1074/jbc.m604035200.

Sonobe H, Yamada R. 2004. Ecdysteroids during early embryonic development in silkworm *Bombyx mori*: metabolism and functions. Zoolog Sci. 21(5):503–516. doi:10.2108/zsj.21.503.

Stoiber M, Celniker S, Cherbas L, Brown B, Cherbas P. 2016. Diverse hormone response networks in 41 independent Drosophila cell lines. G3 (Bethesda). 6(3):683–694. doi:10.1534/g3.115.023366.

Storelli G, Nam H-J, Simcox J, Villanueva CJ, Thummel CS. 2019. Drosophila HNF4 directs a switch in lipid metabolism that supports the transition to adulthood. Dev Cell. 48(2):200–214.e6. doi:10.1016/j.devcel.2018.11.030.

Sun W, Shen Y-H, Qi D-W, Xiang Z-H, Zhang Z. 2012. Molecular cloning and characterization of Ecdysone oxidase and 3--dehydroecdysone-3α-reductase involved in the ecdysone

inactivation pathway of silkworm, *Bombyx mori*. Int J Biol Sci. 8(1): 125–138. doi:10.7150/ijbs.8.125.

Sztal T, Chung H, Berger S, Currie PD, Batterham P, Daborn PJ, 2012. A cytochrome P450 conserved in insects is involved in cuticle formation. PLoS One. 7(5):e36544. doi:10.1371/journal.pone.0036544.

Takeuchi H, Chen J-H, O'Reilly DR, Turner PC, Rees HH. 2001. Regulation of ecdysteroid signaling: cloning and characterization of ecdysone oxidase. J Biol Chem. 276(29):26819–26828. doi:10.1074/jbc.m104291200.

Tawfik AI, Tanaka Y, Tanaka S. 2002. Possible involvement of ecdysteroids in embryonic diapause of *Locusta migratoria*. J Insect Physiol. 48(7):743–749. doi:10.1016/s0022-1910(02)00099-9.

Thompson MJ, Feldlaufer MF, Lozano R, Rees HH, Lusby WR, Svoboda JA, Wilzer KR. 1987. Metabolism of 26-[C-14]hydroxyecdysone 26-phosphate in the tobacco hornworm, *Manduca sexta* L., to a new ecdysteroid conjugate: 26-[C-14]hydroxyecdysone 22-glucoside. Arch Insect Biochem Physiol. 4(1):1–15. doi:10.1002/arch.940040102.

Vigne P, Frelin C. 2010. Hypoxia modifies the feeding preferences of Drosophila. Consequences for diet dependent hypoxic survival. BMC Physiol. 10(1):8. doi:10.1186/1472-6793-10-8.

Wang SF, Ayer S, Segraves WA, Williams DR, Raikhel AS. 2000. Molecular determinants of differential ligand sensitivities of insect ecdysteroid receptors. Mol Cell Biol. 20(11):3870–3879. doi:10.1128/mcb.20.11.3870-3879.2000.

Wang Y, Zuber R, Oehl K, Norum M, Moussian B. 2015. Report on *Drosophila melanogaster* larvae without functional tracheae. J Zool. 296(2):139–145. doi:10.1111/jzo.12226.

Weiszmann R, Hammonds AS, Celniker SE. 2009. Determination of gene expression patterns using high-throughput RNA in situ hybridization to whole-mount Drosophila embryos. Nat Protoc. 4(5): 605–618. doi:10.1038/nprot.2009.55.

Williams DR, Fisher MJ, Smagghe G, Rees HH. 2002. Species specificity of changes in ecdysteroid metabolism in response to ecdysteroid agonists. Pestic Biochem Physiol. 72(2):91–99. doi:10.1006/pest.2001.2588.

Wingen A, Carrera P, Ekaterini Psathaki O, Voelzmann A, Paululat A, Hoch M. 2017. Debris buster is a Drosophila scavenger receptor essential for airway physiology. Dev Biol. 430(1):52–68. doi:10.1016/j.ydbio.2017.08.018.

Wu L, Jia Q, Zhang X, Zhang X, Liu S, Park Y, Feyereisen R, Zhu KY, Ma E, Zhang J. *et al*. 2019. CYP303A1 has a conserved function in adult eclosion in *Locusta migratoria* and *Drosophila melanogaster*. Insect Biochem Mol Biol. 113:103210. doi:10.1016/j.ibmb.2019.103210.

Xu H, Lee S-J, Suzuki E, Dugan KD, Stoddard A, Li H-S, Chodosh LA, Montell C. 2004. A lysosomal tetraspanin associated with retinal degeneration identified via a genome-wide screen. EMBO J. 23(4): 811–822. doi:10.1038/sj.emboj.7600112.

Yamada R, Sonobe H. 2003. Purification, kinetic characterization, and molecular cloning of a novel enzyme ecdysteroid-phosphate phosphatase. J Biol Chem. 278(29):26365–26373. doi:10.1074/jbc.m304158200.

Yamada R, Yamahama Y, Sonobe H. 2005. Release of ecdysteroid-phosphates from egg yolk granules and their dephosphorylation during early embryonic development in silkworm, *Bombyx mori*. Zoolog Sci. 22(2):187–198. doi:10.2108/zsj.22.187.

Yamanaka N, Rewitz KF, O'Connor MB. 2013. Ecdysone control of developmental transitions: lessons from Drosophila research. Annu Rev Entomol. 58(1):497–516. doi:10.1146/annurev-ento-120811-153608.

Zachary D, Hoffmann JA. 1980. Endocrine control of the metamorphosis of the larval muscles in *Calliphora erythrocephala* (Diptera): in vitro studies of the role of ecdysteroids. Dev Biol. 80(1):235–247. doi:10.1016/0012-1606(80)90511-4.

Zhang S, Wu S, Yao R, Wei X, Ohlstein B, Guo Z. 2024. Eclosion muscles secrete ecdysteroids to initiate asymmetric intestinal stem cell division in Drosophila. Dev Cell. 59(1):125–140.e12. doi:10.1016/j.devcel.2023.11.016.

Editor: J. Tennessen